Biomaterials 196 (2019) 2–17

Contents lists available at ScienceDirect

Biomaterials

journal homepage: www.elsevier.com/locate/biomaterials

Emerging trends in multiscale modeling of vascular pathophysiology: Organ-on-a-chip and 3D printing

Karli Gold [a], Akhilesh K. Gaharwar [a, b, c, *], Abhishek Jain [a, **]

[a] Department of Biomedical Engineering, Texas A&M University, College Station, TX, 77843, USA
[b] Department of Material Sciences, Texas A&M University, College Station, TX, 77843, USA
[c] Center for Remote Health and Technologies and Systems, Texas A&M University, College Station, TX, 77843, USA

ARTICLE INFO

Article history:
Received 28 April 2018
Received in revised form
13 July 2018
Accepted 18 July 2018
Available online 23 July 2018

Keywords:
Vascular disease
3D printing
Organ-on-a-chip
Tissue modeling

ABSTRACT

Most biomedical and pharmaceutical research of the human vascular system aims to unravel the complex mechanisms that drive disease progression from molecular to organ levels. The knowledge gained can then be used to innovate diagnostic and treatment strategies which can ultimately be determined precisely for patients. Despite major advancements, current modeling strategies are often limited at identifying, quantifying, and dissecting specific cellular and molecular targets that regulate human vascular diseases. Therefore, development of multiscale modeling approaches are needed that can advance our knowledge and facilitate the design of next-generation therapeutic approaches in vascular diseases. This article critically reviews animal models, static *in vitro* systems, and dynamic *in vitro* culture systems currently used to model vascular diseases. A leading emphasis on the potential of emerging approaches, specifically organ-on-a-chip and three-dimensional (3D) printing, to recapitulate the innate human vascular physiology and anatomy is described. The applications of these approaches and future outlook in designing and screening novel therapeutics are also presented.

1. Introduction

Vascular diseases, such as atherosclerosis, aneurysms, peripheral artery disease, and thrombosis, are the leading cause of morbidity and mortality worldwide, accounting for over 17 million deaths per year [1]. Despite major advancements to develop therapeutic interventions, the pathophysiology as it applies to humans is still largely unclear and treatments limited. If the status quo remains, the number of deaths are projected to reach epidemic proportions by 2030 (>23.6 million) [1]. Thus, there is a crucial need to increase our understanding of vascular disease pathophysiology and assess emerging interventions to accelerate therapeutic development.

In order to model the pathophysiology and influence of various factors (e.g. drug, toxins, biological agents) on vasculature, animal models and cell culture techniques are the current gold standard. The aim of these systems is to recapitulate the biological functions from the subcellular level to whole organs and have contributed immensely to our current understanding of vascular diseases and potential treatments. However, animal model and cell culture techniques do not adequately mimic human *in vivo* microenvironment at these multilevel scales (Fig. 1A). Moreover, these systems do not permit for dissectable analysis of cell signaling mechanisms, therefore limiting their translational potential. Consequently, there is an unmet need to introduce a more predictable vascular disease model. In order to accomplish this, modeling approaches that evaluate molecular, cellular, tissue, and organ level variables are required for a systematic and robust assessment of mechanisms and therapeutic interventions in the blood vessel.

In this review, our focus is on the recent advances in multiscale modeling of vascular pathophysiology. First, the need for modeling pathophysiology of healthy and diseased vascular tissues will be briefly discussed, followed by a critical evaluation of animal models and *in vitro* culture systems. Then we will discuss the potential of organs-on-a-chip and three-dimensional (3D) printing as more predictive modalities, each having distinct positive features but also limitations. For example, the organ-on-a-chip technology is

* Corresponding author. 101 Bizzell Street, ETB 5024, College Station, TX, 77843, USA.
** Corresponding author. 101 Bizzell Street, ETB 5008, College Station, TX, 77843, USA.
E-mail addresses: gaharwar@tamu.edu (A.K. Gaharwar), a.jain@tamu.edu (A. Jain).

https://doi.org/10.1016/j.biomaterials.2018.07.029
0142-9612/

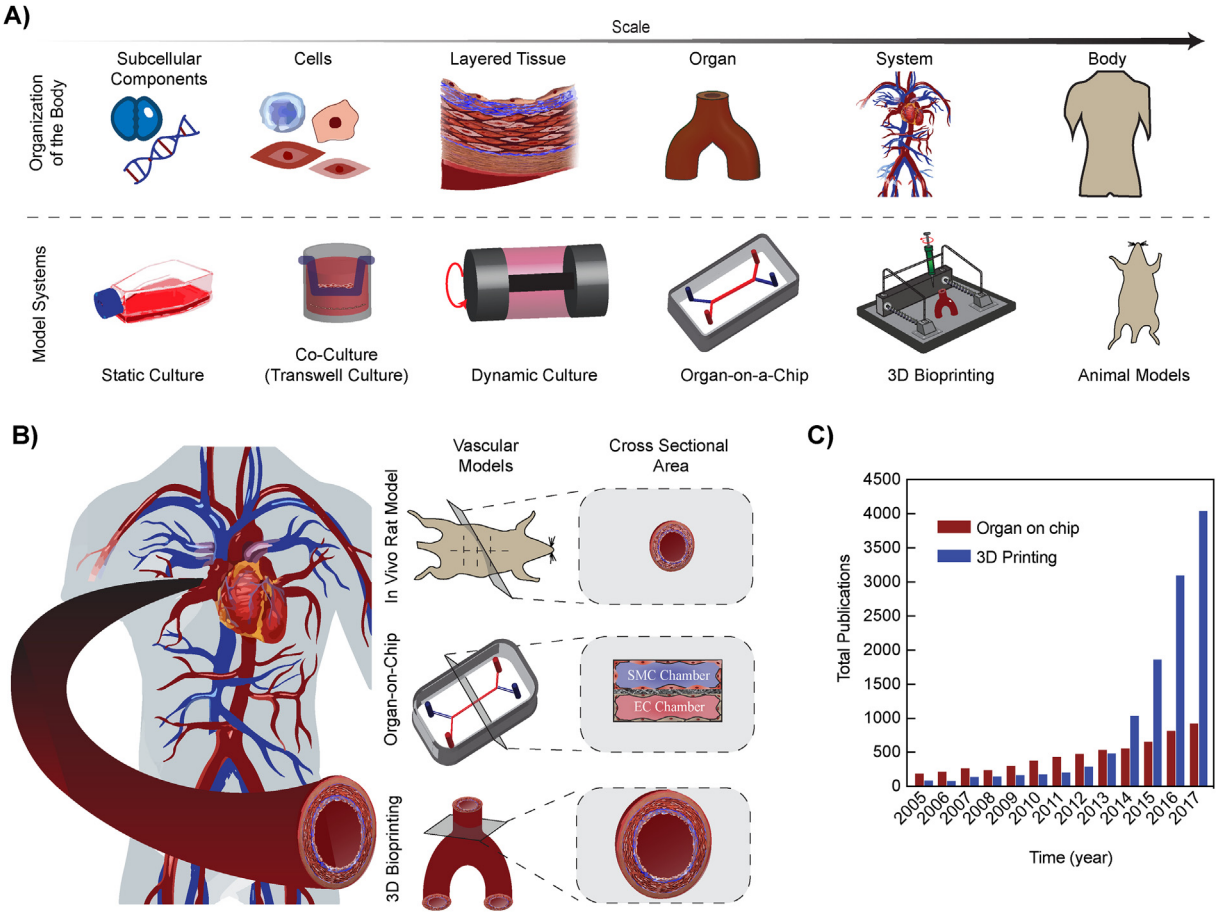

Fig. 1. Existing and emerging multiscale models of vascular diseases. A) Schematic illustrating the model systems used to replicate the organization of the body. As the scale increases from subcellular components to the body, the modeling modalities increase in complexity and decrease in the biochemical tools available to assess the model. **B**) The human vasculature system can be modeled using the standard *in vivo* rodent model (smaller cross-sectional area), organ-on-chip technology (rectangular cross-sectional area), and 3D Bioprinting (mimics the innate human vascular system). **C**) Number of publications related to "vascular models" over the past 12-years, with search keywords "3D Printing or Additive Manufacturing or 3D Bioprinting and Vascular Model" and "Organ-on-chip or Microphysiological System or Tissue chip and Vascular Model" according to ISI Web of Science (Data obtained in July 2018).

able to form tissue-tissue interfaces and combine physiological flow conditions in a variety of disease and organ models. However, these systems often contain a rectangular cross-sectional area, compared to round organs such as blood vessels. Alternatively, 3D printing can produce anatomically accurate vascular anatomy, including bifurcations and curvatures of vascular networks. However, 3D printed constructs are often difficult to integrate optical microscopy, as they cannot be miniaturized to micron sizes. Nevertheless, the unique aspects of organs-on-a-chip and 3D printing techniques are making them increasingly popular tools to understand the pathophysiology and function of patient-specific vascular diseases (Fig. 1B). This is supported by the number of publications pertaining to organ-on-a-chip and 3D printing vascular disease models, undergoing an exponential increase over time (according to ISI Web of Science, July 2018, Fig. 1C). Due to recent advances in the field of biomaterials, microfabrication, and additive manufacturing, we predict that these emerging *in vitro* vascular disease models will advance basic science and serve as a translational platform to design novel therapeutics and repurpose existing drugs.

2. Need for modeling vascular system and pathophysiology

The vascular system is the largest organ system in the body and controls the transport of fluid to and from tissues. The vessels within the circulatory system form a multilayered architecture composed of endothelial cells (ECs), smooth muscle cells (SMCs), fibroblasts, and extracellular matrix (ECM). The innermost, or intima layer, contains a confluent layer of ECs that align with the direction of fluid flow. This layer serves as an active, selectively permeable barrier between the vessel wall and circulating fluids [2]. The tunica media, or middle layer, is predominately composed of SMCs arranged circumferentially around the intima layer, providing structural stability and contractility to control blood flow [2,3]. SMCs deposit collagen bundles around interconnected layered elastin networks, accounting for a majority of arterial mechanical properties [4]. The combination of elastin and collagen provide non-linear elasticity to vessel [5,6]. The outer layer, or adventitia, of blood vessels is composed of fibroblasts and loose connective tissue, serving as an anchor for the vessel [7]. Together, this lamellar structure maintains several biological functions of the blood vessel, such as regulation, extravasation, or intravasation [8].

Vascular diseases result from changes in both structure and function of the blood vessel. For example, arteries may undergo structural changes due to degenerative conditions, infection, or inflammation causing disturbed blood flow [9]. This compromised flow results in an activated endothelium (Fig. 2) [10]. For example in atherosclerosis, once the endothelium becomes activated, it recruits monocytes and leukocytes, and secretes inflammatory chemokines [11]. Prothrombotic mediators are also released,

encouraging platelet activation and SMC proliferation [11,12]. Overall, these functional changes initiate geometrical modifications to the vessel, growing lesions that radially push towards the lumen, decreasing the vascular diameter, causing arterial hardening [6,9,10], and recruiting collagen fibers within the medial layer to support the vessel wall [13,14]. Therefore, the dynamic complexity associated with human vascular diseases, specifically the vascular wall, is extremely difficult to fully recapitulate. However, vascular disease modeling is essential to progress our understanding of disease progression and ultimately, find immediate interventions. A predictable and translatable model includes the cross-talk between essential cellular and tissue components, specifically ECs, SMCs, ECM, and blood constituents under flow. The components needed and models used sets the stage for the biological problem to be solved.

3. Animal models

Animal models have been extensively used to develop our current understanding of vascular diseases and treatment strategies. A major advantage of these systems is that they are able to provide integrated, multi-organ responses to a diverse range of experimental variables (for example, environmental factors, diet, drugs and toxins). Specifically, these models contain multi-cellular and dynamic tissue environments, thus eliciting a whole-body response that can be measured and predicted up to the pre-clinical stage of scientific discovery. For example, animal models have contributed immensely in the discovery of lipid-binding proteins, lipid-transfer proteins, cholesterol transporters, and enzymatic pathways in vascular disease genesis and progression [15,16]. The mechanistic insight gained from animal models has aided in the development of interventions such as, tissue plasminogen activator to eliminate blood clots, several antiplatelet/anticoagulants to reduce the likelihood of blood clot formation, and ion-channel blockers to regulate muscle contraction/arrhythmias [17–19].

While several animal species are utilized, rodent vascular models are most frequently used due to ease of genetic manipulation, breeding, maintenance, cost, and time frame [20,21]. Contemporary molecular and genetic manipulations, such as the creation of hypercholesterolemia apolipoprotein E gene and low-density lipoprotein receptor knockout has humanized mouse models, thus enabling the study of inhibitors on vascular diseases and atherosclerosis with higher precision [19,22]. Nevertheless, rodents exhibit several characteristics that differ from humans, limiting their ability to model human physiology and innate disease development. For example, lesion disruption and lipoprotein content is not identical between humans and mice [23]. Vessel sizes, blood composition, and biophysical properties exhibited by rodents can be vastly different from humans, thus providing poor predictive value to disease outcomes. Given such large discrepancies between these two species, large animal studies are often required even if rodent models are used.

Large animal models (i.e. porcine, rabbits, baboons, non-human primates), being closer in anatomy and genetic composition to humans, are used in advanced preclinical trials to model complex signaling pathways of vascular diseases and drug responses. The large size of these animals provides an increased tissue availability for histopathological analysis and facilitates non-invasive measurements, such as measuring vascular hemodynamics [24]. In addition, these models provide a more accurate representation of human metabolism and vascular anatomy (heart size and coronary circulation) [22]. Therefore, large animal models have thus far, predominately contributed to the drug discovery process in vascular diseases [23,25]. However, large animals cannot easily undergo genetic modifications, thus their translational potential diminishes [26]. Furthermore, it is extremely difficult to dissect specific signaling pathways and analyze tissue-tissue or cell-cell interactions independent of other factors. To overcome the

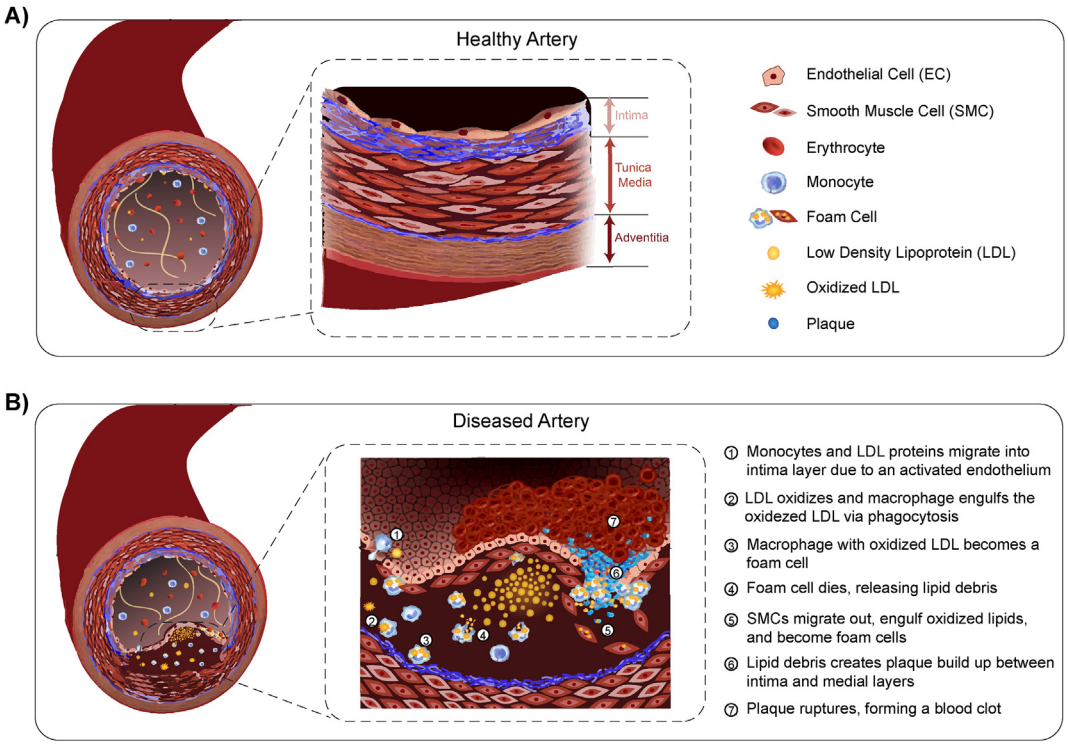

Fig. 2. Complex composition of an artery A) Basic anatomy of a healthy, human arterial blood vessel, containing the intima, tunica media, and adventitia layer. **B)** Illustration of the complex pathophysiological development and progression of vascular disease causing a structural and functional change in arteries.

Table 1
Advantages and Limitations of animal models of vascular diseases.

	Rodent Models	Large Animal Models	Non-human Primates
Advantages	+ Ease of genetic manipulation, breeding, costs and time frame	+ Close to human anatomy (i.e. hear size and coronary circulation) + Close to human genetic composition (i.e. lipoprotein metabolism, enzymatic activity, cholesterol distribution) + Circulating volumes reflect similar volumes to humans + Increased tissue availability + Facilitates in collection of non-invasive measurements	+ Phylogenetically closest to humans (i.e. analogous diet, metabolism) + Develop vascular disease with age + Close to human genetic composition (i.e. lipoprotein metabolism, enzymatic activity, cholesterol distribution) + Increased tissue availability + Facilitates in collection of non-invasive measurements
Limitations	– Compromised lesion development – Varied anatomy – Increased heart rate – Diverse lipoprotein ranges – No expression of cholesteryl ester transfer protein – Inability and infrequency of plaque rupture and thrombosis	– Restrictions on genetic manipulations to mimic human physiology – Difficult to extrapolate, interpret, and relate data to humans – Difficult to isolate relevant tissues/cells for experimental response – Inability and infrequency of plaque rupture and thrombosis	– Significant restrictions due to ethical concerns – Threat to maintain biodiversity – Require long-term experimentation

anatomical and physiological limitations of rodent and large animal models, non-human primates serve as ideal candidates who most closely reflect the innate biological processes within human vascular systems. Non-human primates (i.e. chimpanzees, baboons) are phylogenetically closest to humans, having analogous diet, metabolism, and development of vascular disease as they age [27–29]. However, use of non-human primates contain significant ethical restrictions and pose as a threat to maintaining biodiversity, therefore limiting their clinical practice [27].

In summary, animal models are able to provide full cellular compositions and complexities observed in human blood vessels, making them an indispensable tool in vascular disease modeling. However, the results obtained from animal models can be difficult to extrapolate, interpret, and do not always relate to human pathophysiology, limiting the translation potential of these models (Table 1). As a result, bioengineered *in vitro* approaches, containing human-derived living cells within relevant microenvironments complement animal models and perhaps, even remove their need in the future.

4. *In vitro* models

While animal models provide a top-down modeling approach, *in vitro* models offer a bottom-up approach to model complex pathophysiology of vascular disease [30]. As a result, *in vitro* models allow the examination of specific cellular and molecular signaling events under defined chemical and mechanical conditions, thus making them an easily tunable system with reduced complexity. *In vitro* models can be static cultures of cells or include complex dynamic motions mimicking the *in vivo* environment more closely. However, both these approaches have advantages and limitations, specifically depending upon the purpose of application.

4.1. Static in vitro culture systems

Since endothelial cells (ECs) line the walls of all blood vessels in circulation and are central to vascular function, most *in vitro* models analyze vascular diseases with EC monolayers [31–39]. Static well-plate systems with monoculture of ECs are simple to use and can be multiplexed. As a result, these systems have become the gold standard to understand endothelial biology [40], responses to internal or external environment changes [41–47], and for high throughput screening applications [17,48].

Nevertheless, blood vessels are multicellular organs, containing external layers of SMCs, fibroblasts, epithelial cells, and embedded ECM. Several cadherin and integrin interactions occur within this lamellar structure that regulate cell behavior [7,17,49–52]. For example, ECs within the intima layer interacts with SMCs in the media layer. This interaction controls the upregulation of inflammatory cytokine expression (i.e. interleukin-8, IL-8, and monocyte chemotactic protein-1, MCP-1) and platelet-derived growth factor (PDGF), while inhibiting collagen and fibroblasts growth factor [50]. These cell-cell and cell-ECM interactions are critical for maintenance of proper blood vessel function. In order to achieve these EC-SMC cadherin interactions, various static co-culture systems have been utilized [48,53–55]. Co-culturing ECs and SMCs have shown mutual physical interactions which impact cell morphology, proliferation rate, and protein synthesis through the excretion of diffusible mediators [48,53,55].

Despite frequent use, monoculture or co-culture well-plate systems cannot recapitulate the complex, dynamic intercellular and organ-level signaling experienced by blood vessels. This is mainly due to changes from a natural 3D tissue environment to a 2D tissue culture, where the cells become exposed to a significantly altered microenvironment (e.g. surface stiffness, biochemical composition, local cell density) [56]. As a result, these static systems can also alter cell phenotype thus reducing the predictive power of these systems [14,56]. For example, SMCs lose contractile proteins upon culture, rendering them incapable to modulate vascular tone [50]. Furthermore, static cultures cannot incorporate shear-dependent cell and tissue responses. For example, when the lumen is subjected to pulsatile blood flow, ECs respond through shear-sensitive ligands and integrins communicating with other regions of the vessel that respond to these signals. ECs respond to changes in shear by secreting or metabolizing vasoactive substances, such as nitric oxide and/or endothelin-1, inhibiting or exciting SMC growth, vasoconstriction, or vasodilation. These perturbations are impossible to mimic in 2D culture assays and therefore, flow-based culture systems are required to undertake such investigations.

4.2. Dynamic in vitro culture systems

In order to integrate mechanical forces to *in vitro* cell culture systems, parallel plate or two-dimensional perfusion flow

chambers have been extensively used [57,58]. Traditional flow chambers are hollow conduits that provide a means to expose EC monolayers to fluidic forces on the millimeter scale, thus making it possible for the assessment of biophysical alterations involved in vascular disease [59–61]. However, due to the large volume of the conduit, these techniques consume large amounts of medium, bioactive factors, and cells. Moreover, these macroscale devices do not represent the microphysiological environment of the smaller blood vessels, such as arterioles or capillaries. Recently, advances in microfabrication techniques have enabled rapid manufacturing of micron-scale flow chambers, termed microfluidic devices. These devices provide a reproducible and low-consumption platform to more precisely control biological conditions and the dynamic fluid environment relevant to arterial blood vessels and vascular diseases [62,63]. A salient feature of microfluidic devices is that they allow quantitative assessment of hematological and microvascular processes of vascular disease. For example, a broad range of velocities that exists in the vascular system - ranging from 0.3 m/s in the aorta to 0.1 μm/s in vascular branches at the capillary level [64] - can be applied within microfluidic devices, thus enabling assessment of the diverse shear-dependent signaling within the endothelium. In addition, flow perfusion provides a mechanism to continuously transport and distribute soluble factors, permitting long term culture of cells and providing a resource to model physical influences on cells (such as the rolling, decelerations, and arrests of blood-components with the endothelium) [65]. Overall, microfluidic methods have shown that they can be used to study whole-cell responses rather than individual mechano-receptors [66,67]. A major advantage of this platform is that it can also include parenchymal cells and ECM, enabling for a method to model complex epithelial-endothelial-blood signaling that occurs in vascular disease, thus functioning as organs-on-a-chip or microphysiological systems.

5. Emerging approaches

From existing animal models and *in vitro* systems, a major hurdle in vascular science and the drug discovery process is the inability of these techniques to reliably predict therapeutic targets and toxicities applicable to humans. As a result, major successes in pre-clinical trials have resulted in failures when translating to human clinical trials. A key reason for this problem is that the current model systems do not recapitulate organ-level architectures and functions critical to the assessment of drugs, toxins and chemicals at a disease-and patient-specific level in humans. Therefore, there is a necessity for new disease models to emerge. With the advent of easy microfabrication methods, automated instrumentation, new biocompatible materials, stem cell differentiation to defined cell lineages, and molecular tools, microfluidic organ-on-a-chip devices and 3D printing have spurred new innovation and shown strong potential to address this unmet challenge. These emerging approaches to model vascular disease provides a unique solution by increasing the translational potential to humans and decreasing the mechanistic complexity associated with the experimental outputs. For example, microfluidic organ-on-a-chip devices can provide biological insight into pathophysiology by providing direct access via microscopy, biosensors, and genomic screening. In contrast, 3D printing can be used to fabricate a patient specific vascular disease model by recapitulating the structural and functional aspects of native tissues.

5.1. Organ-on-a-chip

Recently, a new class of microfluidic devices known as organ-on-a-chip, or microphysiological systems has emerged and shown to recapitulate 3D tissue architectures and physiological flow conditions in a variety of disease and organ models. These systems have recreated the microenvironment of lung, liver, gut, kidney, skin, intestine and many other organs [56,68–73], where cadherin interactions, tissue-tissue communication, and mechanical stimulation of fluids can be controlled in a physiologically-relevant manner not possible with animal models or classic *in vitro* systems. Organ-on-a-chip is broadly defined by the minimum assembly of cells in a microenvironment that mimics organ-level function of a human. Importantly, this platform can include the endothelial lumen, blood flow in complex vascular geometries (such as, stenosis, aneurisms and bifurcations) and the inclusion of mechanical forces that govern endothelial activation can be included (Fig. 3A). This inclusion offers enormous potential to model vascular disease mechanisms with higher specificity and accuracy not offered by conventional methods (Table 2).

Recent studies have shown that atherothrombotic processes and platelet aggregation can be modeled with the organ-on-a-chip platform [70,74,75]. In one such study, a microfluidic device containing a parallel array of stenosed microvessels was able to form platelet and fibrin-rich blood clots downstream of stenosis, as observed *in vivo* [72]. This device was then applied to predict anticoagulant and antiplatelet drug responses in patients on extracorporeal devices (Fig. 3B). Another *in vitro* study applying a similar geometry validated that cell-secreted von Willebrand Factor (VWF) further exacerbates platelet recruitment and adhesion post-stenosis, like *in vivo* [31]. In another study, a microfluidic channel (vessel-on-a-chip) lined with living or chemically fixed human endothelium was demonstrated to maintain its ability to modulate hemostasis and thrombosis under arterial flow, thus serving as a potential diagnostic lab-on-a-chip device (Fig. 3C) [70,76]. More recently, this vessel-on-a-chip system was able to predict toxicity of a drug compound that failed clinical trials but did not produce the same vascular side-effects in primate studies [77]. Also, this organ-on-a-chip platform has provided more mechanistic understanding of vascular biology. For example, a recent work with microfluidic channels showed that proteins RhoA, Rac1, and N-cadherin regulate vascular permeability and barrier function [78]. Furthermore, immune cell interactions have also been assessed in these systems, demonstrating the role of inflammatory cells, such as neutrophils and T-cells, play on endothelium activation and consequent thrombosis formation [79–81].

More complex diseases, such as, cancer, infectious diseases and several genetic disorders, like sickle cell disease, result in vascular problems in patients and often, such patients encounter fatal strokes. Tissue and cell signaling in such diseases may constitute feedback between multiple organs and epithelial that regulate vascular function. For example, in cancer, the tumor cells release inflammatory factors that result in vascular dysfunction [38]. Similarly, in pneumonia and other respiratory disorders, the alveolar epithelium may secrete factors that lead to platelet recruitment and thrombosis [39]. Organ-on-a-chip technology has been deployed to dissect tissue-tissue and drug-tissue interactions for systematic analysis of such complex vascular diseases. Recently, a model of lung thrombosis supported organ-level functional design by showing co-culture of human primary alveolar and endothelial lumen in adjacent microfluidic conduits, separated by thin layer of matrix [26]. When human whole blood was perfused through this lung thrombosis device, after introduction of lipopolysaccharide (LPS) in the abluminal epithelial compartment, thrombus formed in the luminal compartment, as found identical to *in vivo* conditions. Further, an endothelium-specific therapeutic effect of an antithrombotic compound was identified with this system, which was not possible to be found using traditional animal models. These recent developments in vascular microphysiological systems are

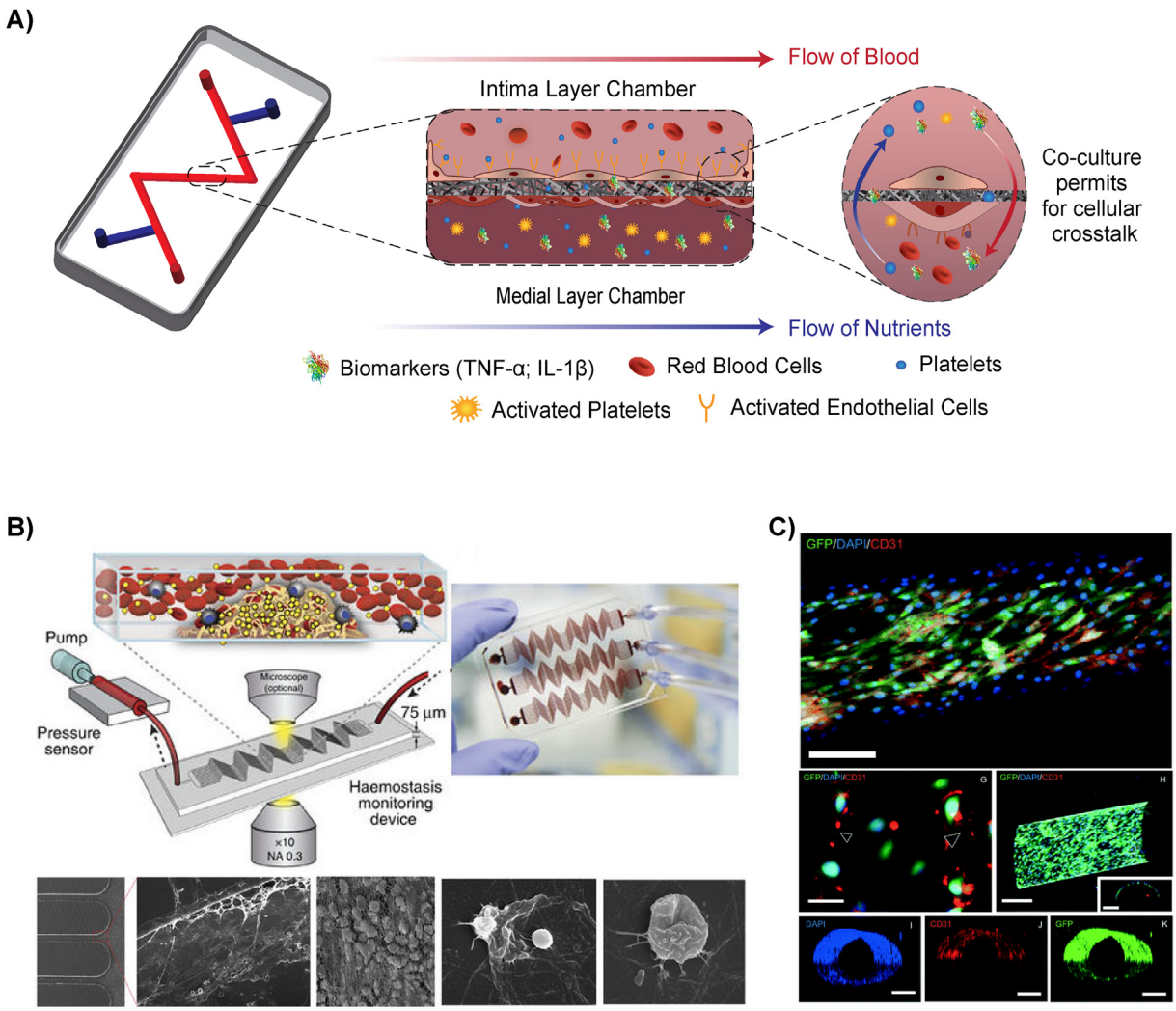

Fig. 3. Vascular organ-on-a-chip models. A) Illustration depicting the cellular communication and dynamic environment within a multi-chamber organ-on-a-chip. **B**) Schematic depicting a hemostasis organ-on-a-chip device, top left. Exposure of blood flow within the microfluidic channel permits for determination of clotting time and the high throughput potential of organ-on-a-chip devices. Scanning electron micrographs of blood clot formation within the device, bottom, illustrating fibrin networks with red blood cell (3 left images) and activated platelets (2 images at right) [72]. © 2016 Nature Communications **C**) Confocal image of GFP/DAPI/CD31 biomarkers from endothelial cell monolayer inside microchannel, depicting cellular interactions. (Top – Scale bar 250 μm; G – Scale bar 50 μm; H, I, J, and K – Scale bar 250 μm) [76] © 2014 Lab on Chip.

highly promising and provide major opportunities to visualize biological functions using microscopy, measure variables using biosensors, and quantified using analytical algorithms and genomic screening.

However, there are still some limitations in the current microfluidic designs that restrict the extent to which vascular disease pathophysiology can be reconstructed. Virtually most published literature on organ-on-a-chip is based on the use of polydimethylsiloxane (PDMS) as the material of fabrication. The process of fabrication with PDMS, called soft lithography, is simple and adoptable to most lab environments. With soft lithography, multichamber microfluidic devices separated by thin film membranes to support tissue co-cultures can be designed with high fidelity. PDMS is also biocompatible, transparent, and permeable to gases, making it very suitable for cell culture. However, a major drawback of PDMS is that the material adsorbs small hydrophobic molecules, therefore making it very difficult to assess pharmacokinetics of drugs and toxins. For example, if the drug is absorbed by the PDMS, then its net concentration is lower, and potential therapeutic effect or toxicity might be underestimated. Thermoplastic materials are potential alternatives that have been used to make microfluidic chips, but they often auto-fluoresce during imaging, do not permit oxygen diffuse (making it harder for cells to survive for long durations), and can be very expensive for a high-throughput setting. Another potential limitation is that organ-on-a-chip models are subsets of the whole living organ. For example, the blood vessel-on-a-chip models published so far lack connective tissue, containing fibroblasts between the epithelium and endothelium, which may regulate vascular homeostasis and pathogenesis. In addition, pericytes or SMCs may need to be integrated under the endothelium for a complete biological output from these models. This is not necessarily a drawback because scientists can design the simplest model and then add additional complexity until the required combination is achieved for solving the problem of interest. For example, blood flow in arteries is pulsatile and will be a very interesting addition to vascular organ-on-a-chip technologies in the future. A major hurdle that still exists is that the cells used in these model systems may not always represent the phenotype of the local environment of the human disease or patient, and therefore, standardization of the cell-lines and growth protocols is necessary [30,82,83]. In addition, given the planar and thin (<1 mm in thickness) cellular arrangement, modeling drug-tissue

Table 2
Bioengineered vascular disease models using organ-on-a-chip technology.

Material	Cell Type(s)	Blood flow conditions	Experiment	Ref.
PDMS	Mouse olfactory harvested arterial segments	Perfusion inlet was subjected to 45 mmHg and the outlet at atmospheric pressure.	Artery segments were reversibly loaded onto device; verified cellular arrangement of artery in chip by staining SMC nuclei, actin, and voltage gated calcium channels; vessel constriction was reduced by 50% after incubating with calcium-blocker nifedipine	Yasotharan et al. [68]
PDMS coated with VWF/fibrinogen	HUVECs	Parallel microchannels with one-side stenosis of 20, 30, 40, 60, or 80 percent lumen reduction; human blood was perfused at 1000 s^{-1} input wall shear rates	Stenotic chambers demonstrated enhanced platelet aggregation in 60–80% occlusion over a range of input wall shear rates; flow increases EC VWF secretion in stenotic outlet, causing platelet aggregation and post-stenotic thrombus formation	Westein et al. [74]
Gelatin-Agarose IPN	HUVECs, HDMVECs, HLMVECs	Physiologically relevant stiffness ~ 20 kPa (stiffness of healthy arteries between 1 and 35 kPa); Flow velocity in smallest channels set to ~2.8 mm s^{-1} (corresponding to a wall shear stress ~8.8 dynes cm^{-2})	Stiffer IPNs (~50 kPa) resulted in increased permeability compared to soft devices (~5 kPa); Extracellular haem (haemolytic by-product) induces delayed and reversible EC permeability (dose-dependent manner)	Qui et al. [164]
PDMS and collagen	hBMSCs, hFs, HUVECs, HASMCs	No profusion mentioned	Inflammatory factors (LPS, thrombin, and TNFα) compromises EC barrier function; Simultaneous inhibition of Rac1and activation of RhoA induced loss of HASMC exposure to HUVECs and reduced barrier function; CRISPR-mediated knockout of *N*-cadherin in HASMCs led to loss of barrier function and over expression in HUVECs *N*-cadherin (validated in mouse model)	Alimperti et al. [165]
PDMS coated with collagen	HUVECs	Perfused human citrated whole blood at a flow rate of 0.29 mL min^{-1}, yielding a shear rate of ~1000 s^{-1}	SLA printed miniaturized vascular structures that closely mimic stenotic and healthy blood vessel architecture; 15 min of blood perfusion revealed induced thrombosis down stream and at the stenotic regions whereas healthy geometries showed no platelet adhesion	Costa et al. [161]
PDMS	Resistance arteries isolated from wile type CD1 mice or CD1 mice expressing Tie2-GFP transgene in ECs	Harvested arteries were fixed at periphery and subjected to external pressure of 45 mmHg above atmosphere (aligned artery); Disk of sapphire uniformly distributed heat generated by thermoelectric heater; Flow in channels between 0 and 4 mL h^{-1}	Developed a microfluidic platform to assess resistance artery structure and function; fully automated acquisition of up to ten does-response sequences of intact mouse mesenteric artery segments; Exposure of phenylephrine or acetylcholine yield dose-response relationship identical to human response	Gűnther et al. [166]
PDMS	HUVECs, HMVEC	Citrated human blood was perfused to obtain a wall shear rate of 750 sec^{-1} (~10 dynes cm^{-2} stress); for platelet-endothelial dynamics, higher wall shear rate was used (750 sec^{-1}; ~30 dynes cm^{-2} stress)	Performed quantitative analysis of organ-level contributions to inflammation-induced thrombosis; LPS endotoxin directly stimulates intravascular thrombosis by activated alveolar epithelium; analyzed inhibition of EC activation and thrombosis due to PAR = 1 antagonist	Jain et al. [167]
Fibronectin crosslinked gelatin	iPSC, NRVMs	Bulk elastic modulus of ca 50–100 kPa; lower concentrations obtained modulus between 1 and 15 kPa	Micropatterned gelatin hydrogels using laser-etching to obtain surface grooves and pillar structures with a resolution of 15 μm; verified structural organization, contractile function, and long-term viability compared to manually patterned gelatin substrates	Janna et al. [168]
PDMS	HAECs and HASMCs	Vacuum side channels induce cyclic strain of 5–8% to mimic stretching and relaxation of the channels; flow in EC chamber produced a wall shear stress of 1–1.5 PA	Culture of SMCs and EC with a porous membrane separating the two chambers lead to prolonged viability of cells that exhibited physiological morphology and organization through cell-cell contact;	Engeland et al. [169]

Abbreviations IPN, inter-penetrating network; HUVECs, human umbilical vein endothelial cells; HDMVECs, human dermal microvascular endothelial cells; HDMVECs, human lung microvascular endothelial cells; PDMS, poly(dimethylsiloxane); hBMSCs, human bone marrow stromal cells; hFs, human lung fibroblasts; HASMCs, human aortic smooth muscle cells; LPS, lipopolysaccharides; HMVEC, human lung microvascular endothelial cells; PAR-1, protease activated receptor-1; iPSC, induced pluripotent stem cells derived cardiomyocytes; NRVMs, neonatal rat ventricular myocytes.

interactions may be inaccurate and require careful scaling up due to varied drug pharmacokinetics and pharmacodynamics [35,56,84–87]. Also, organ-on-a-chip models may not always include the same cellular arrangements as *in vivo*. They are often designed as overlaying or side-by-side rectangular channels which make them unable to recapitulate the exact flow inside a cylindrical blood vessel. This may also alter endothelial function and affect the contractility-related mechanisms of cells. Finally, despite promising use of organ-on-a-chip, these models may not be appropriate to model the macroscale organ biology, for example, aorta or veins and therefore, different tools may be needed for such investigations.

5.2. 3D printing

Given that vascular diseases often originate in blood vessels with complex geometries, additive manufacturing, such as 3D printing (including 3D bioprinting), offers a vital tool to recapitulate a diseased anatomy. 3D printing is a fabrication technique used to mimic the anatomical complexity of native tissue, *via* a bottom-up approach, by depositing polymeric or cell-laden hydrogel based inks, in a layer-by-layer fashion (Fig. 4A) [88,89]. The use of 3D printing to fabricate intricate geometries, such as bifurcations and curvatures, provides a comprehensive understanding and functional evaluation of patient-specific vascular disease symptoms

[90,91] (Table 3). Recent advancements in 3D printing technology has resulted in the development of complex, anatomical structures, motivating its use in a variety of biomedical applications such as tissue modeling [92–94], pharmacological assessment of therapeutics (contractions of vascular wall in response to serotonin [95], endothelin-1 [95–97], prostaglandin $F_2\alpha$ [95], polyphenols from red wine [98,99], and histamine [100]), and disease pathophysiology (neovascularization [101] EC permeability [102,103], and hemodynamics [104,105]).

A vital yet limiting component of the 3D printing design and implementation is the selection of materials, or bioinks. The materials used serve as an artificial ECM composed of natural, synthetic, or their combination to reproduce tissue microenvironments and permit for cellular functions observed on native ECM. Natural polymers encompass materials derived from natural sources, such as ECM constituents (e.g. collagen, elastin, and fibrin) or polysaccharide-based biomaterials (e.g. alginate, chitosan) [106–108]. These materials often contain cell-adhesive domains, driving for cell adhesion, migration, and proliferation. However, natural polymers often contain significant batch-to-batch variability, as well as a lack of control over the chemical and physical properties. To overcome the variability of natural polymers, synthetic polymers with desired chemical structures, mechanical integrity and functionality are used [109,110]. However, synthetic materials lack biological recognition domains, resulting in limited cell-matrix interactions. In order to enhance or obtain bioactivity, synthetic polymers are modified with cell-responsive structures, such as RGD-domains or natural polymers. Due to the inherent complexity of vascular tissue, combining both natural and synthetic polymers warrant for the fabrication of bioinks that can be finely tuned to obtain optimal material properties and enhanced bioactivity [111,112]. The combination of both natural and synthetic polymers to fabricate vascular constructs enables for precise manipulations to model tissue compositions, architectures, and microenvironments in healthy and diseased conditions [113–115]. This permits for dissectible analysis of physiological changes that occurs with geometry, disease progression, and ageing [112,116].

In order to further recapitulate ECM properties of vascular tissues, such as conductivity, nanomaterials such as carbon nanotubes [117,118], graphene oxide [119], and gold nanorods [120] can be integrated into polymeric networks. These nanomaterials can also be used to modify a materials printability to fabricate anatomically scaled tissue structures that are able to model the macroscale organ biology. In a recent study, anatomically accurate bifurcating vascular constructs were 3D printed with precise geometries (Fig. 4B) [114,121]. In this approach, bioink properties were optimized by controlling the interaction between nanoparticles and polymeric network to obtain highly printable inks [113,121–124]. Printability is a crucial property of bioinks that is defined by its ability to smoothly extrude into the intended architecture with high structural fidelity. These properties are governed by a materials rheological properties and crosslinking mechanisms [125]. Specifically, a bioink must first shear-thin, allowing for extrusion through a needle gauge, followed by rapid recoverability of the material's internal structure, permitting for shape retention into the deposited geometry [113]. A range of approaches have been developed to print custom scaffolds with enhanced fidelity, such as on-site curing of bioink [126,127], printing into support bath [128–131], or exposing ions or temperature changes to retain a deposited shape [114,121].

Aside from print fidelity, bioink selection is crucial as it can dictate cellular organization and functions. By modulating bioink properties, biophysical and biochemical microenvironments of human vascular diseases can be recapitulated [132]. For example, recent studies have utilized 3D printing to design a cardiac patch by mimicking the cardiac niche-like microenvironment in order to improve cardiomyocyte organization and maturity (Fig. 4C) [133,134]. This 3D printed model was able to produce physiological responses to a androgen agonists (such as epinephrine; Epi - increases heartbeat frequency) and carbachol (CCH; decreases heartbeat frequency) [135]. In a similar study, 3D printing was used to fabricate constructs with specific surface topography to control cellular adhesion and alignment (Fig. 4D) [136,137]. This approach is capable of mimicking some of the structural complexity observed with native vasculature. These proof-of-concept studies highlight the versatility of 3D bioprinting to mimic structural and functional complexity of vascular tissues.

Although printing design has been used to dictate cellular arrangement on printed scaffolds, construct topography, stiffness, and architecture also strongly impact the model's predictability, specifically regarding the devices hemocompatibility. In healthy vasculature, blood does not clot due to a confluent layer of EC shielding the ECM from fluid contact fluid [138]. The ECs prevent clotting through the release of biochemical ques to the blood, such as heparans, thrombomodulin, tissue plasminogen activator, and adhesion proteins to dictate vascular function [139]. However, when the lumen is disrupted or damaged, the underlying ECM elicits highly thrombogenic properties, triggering immediate platelet adhesion and thrombosis [9,140]. Bioink properties can be tuned to prevent this clotting cascade and improve upon the ink's hemocompatibility. Specifically, sub-micrometer rigids and grooves on the blood-contacting surface has been shown to decreases platelet adhesion and activation compared to smooth surfaces [141–143]. This is due to an increased surface area and geometrical constraints for platelet adhesion and activation. In addition, increased matrix stiffness (~5–50 kPa) has been shown to significantly enhance platelet adhesion and spreading, *via* Rac 1 and actomyosin activity [144–146]. Aside from surface roughness and matrix stiffness, other strategies, such as the inclusion thrombosis resistant materials [147,148] or chemical modifications of the constructs surface [149,150] greatly impact platelet interactions with the model.

3D printing can also be combined with other fabrication techniques, such as solution blow spinning, photolithography, or self-assembly to imitate more complex structural features of vascular tissues. For example, innate myocardium ECM consists of a well-organized, anisotropic tissue with conductive fibers [151,152]. Electrospinning, an electrostatic fabrication technique to obtain micro- and nano-fibers, can be used to mimic structural organization of myocardium ECM by providing topological clue for cell alignment and impart directional properties. By combining electrospinning with 3D printing, a patient-specific vascular graft can be obtained (Fig. 4E), which is difficult to obtained from either technique alone [153]. The topological clue provided by electrospun fibers facilitate formation of vascular tissue around the graft *in vivo* after 6 weeks. Interesting, the secreted ECM consists of predominantly collagen and elastin, which are similar to the native inferior vena cava. In addition, there was no observable calcification of the engineered graft [153]. This study indicated strong potential of combining 3D printing with other fabrication techniques such as electrospinning to mimic structural complexity of vascular anatomy. Aside from combining with other fabrication techniques, 3D printing has recently been used for a template micro molding technique (Fig. 4F) [76]. Complex vascular microchannels can be printed out of a sacrificial bioink, such as agarose [76], gelatin [154], or pluronics [106,155,156]. After the printed microchannels gel cooler temperatures, a cell-laden hydrogel precursor solution can be caster over the fibers and photo-crosslinked. Subsequently, the sacrificial microchannel templates are removed from the surrounding crosslinked hydrogel by increasing past the materials

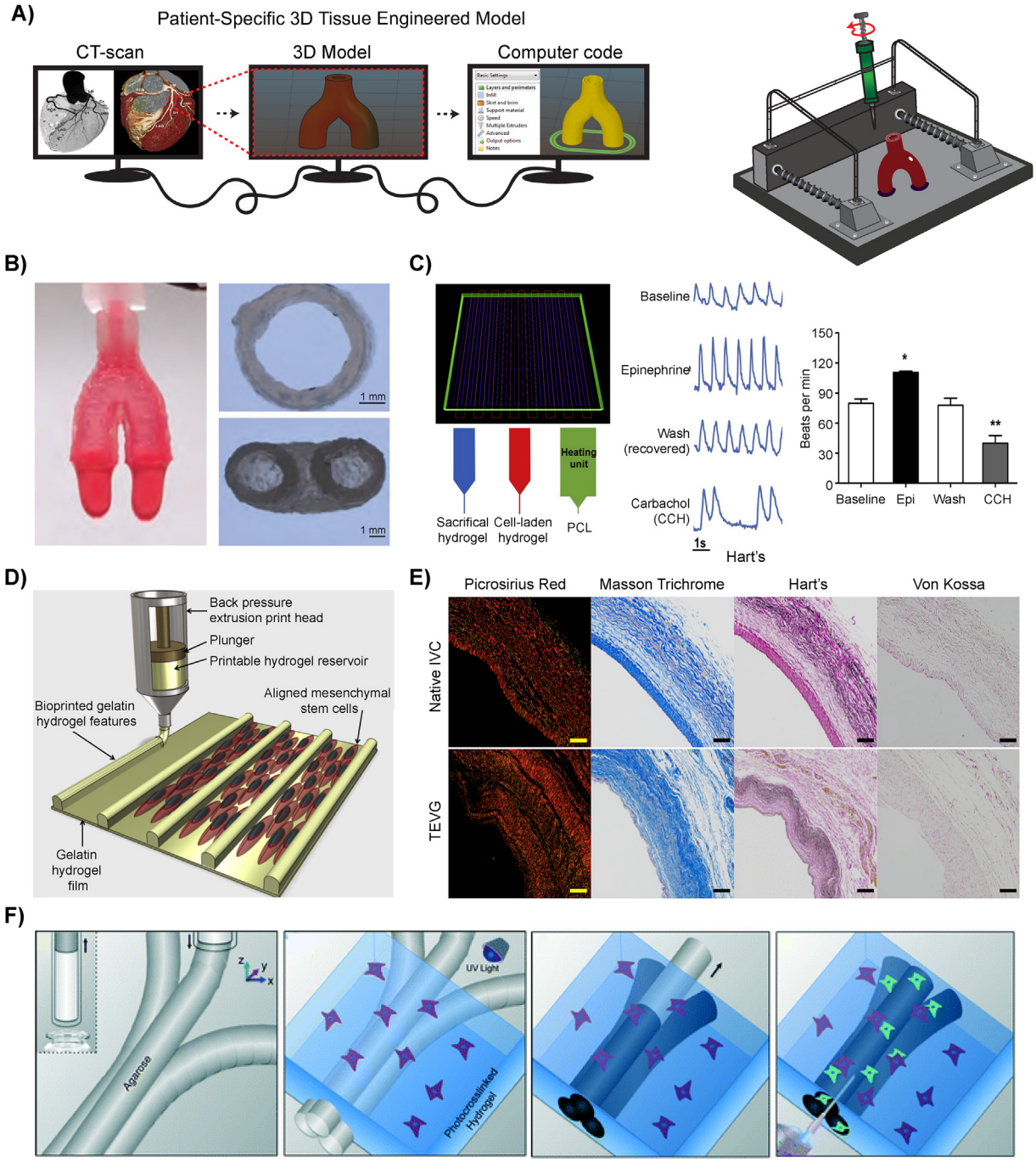

Fig. 4. Vascular 3D printed models. A) Schematic demonstrating the process of fabricating a patient-specific complex geometry using the layer-by-layer 3D printing process. **B**) A bioink utilizing Nanoengineered Ionic-Covalent Entanglements (NICE) improves the hydrogels printability, producingstiff and elastomeric constructs that are physiologically relevant at modeling macroscale organ biology [114]. © 2018 ACS Applied Materials & Interfaces **C**) 3D printing of 3-component cardiac tissue to demonstrate the feasibility of cardiac model drug response. The printed cardiac tissue increased in beating frequency (beats per minute; BPM) and amplitude, compared to the baseline, when exposed to epinephrine (Epi). However, once removed, washed, established baseline, and then exposed to Carbachol (CCH), the opposite effect was confirmed [137]. © 2018 Acta Biomaterialia **D)** Schematic of the manufacturing process used to produce hydrogel printed microchannels that aid in cellular alignment, mimicking the arrangement observed *in vivo* [136]. © 2018 Biofabrication **E)** Collagen (Picrosirius Red and Masson Trichrome) and elastin (Hart) deposition of a native inferior vena cava (IVC) compared to a 3D printed tissue engineered vascular graft (TEVG) after 6 months. No signs of ectopic calcification were demonstrated (Von Kossa) [153]. © 2017 The Journal of Thoracic and Cardiovascular Surgery **F)** Graphic representation of the use of 3D printing to form microchannels *via* template micro-molding, permitting for the use of dynamic co-culture within a printed construct [76]. © 2014 Lab on chip.

melting temperature. This fabrication technique enables the fabrication of anatomically accurate, perfusable microchannels and permit for co-culture of multiple cell types. The use of sacrificial material 3D printing provides a platform to create a fully perfusable microvascular network with different architectures and geometries.

Although 3D printed constructs are capable of mimicking the native structure of blood vessels and can model several aspects of vascular diseases, few significant hurdles still remain before this technology can be translated to preclinical trials or medical

Table 3
Bioengineered vascular disease models using 3D printing technology.

Material	Cell Type(s)	Mechanical Conditions	Experimental Specifications	Ref.
GelMA for bulk material and Pluronic F-123 for sacrificial microchannels	HUVECs, hDFs	Reynolds number lower than 0.5 for flow rates between 0.6 and 3 mL h^{-1} (laminar flow); main velocities in main channel between 0.19 and 0.54 mm s^{-1}; burst pressure: ~0.16 ± 0.08 kPa; Compression moduli varied between 0.8 kPa to 0.65 kPa	Sacrifical bioprinting produced hDF encapsulated in GelMA with microchannels (washed out pluronic) devices lined with a confluent layer of HUVECs; profusion of blood formed thrombi that was exposed to tissue plasmin activator and subsequent dissolution of non-fibrotic clots; hDF were able to migrate into the clot and deposited collagen over time	Zhang et al. [75]
Nanosilicates, GelMA, kappa-carrageenan	MC 3T3 Preosteoblasts	Addition of nanosilicates to the network induces a Herschel-Bulkley fluidic behavior, promoting a shear thinning profile with a power law index of 0.55	Utilized a ionic and covalent network stabilized by nanosilicates to produce high fidelity printed constructs; performed rheological modeling to determine optimal parameters for printing	Chimene et al. [114]
PEGDA, Alginate	PAVIC	Alginate was incorporated into bioink to increase precursor viscosity to permit for printing of high fidelity constructs; Lower weight percent of bioink had increased linear elasticity behavior, higher weight percent bioink exhibited nonlinear tensile stress-strain behavior	3D printing and photo-crosslinking technique to construct heterogeneous aortic valve to mimic the anatomic and axisymmetric geometries	Hockaday et al. [115]
Alginate, Collagen	Mouse fibroblasts, mouse SMCs, and HUVECs	Construct exhibited a linear stress-strain profile with an ultimate strength increases with increasing alginate concentration (0.049 MPa–0.139 MPa); After 5 days of culture, the ultimate tensile strength decreased further to 0.105 MPa	3D printing of multi-level fluidic channels deposited in a layer fashion to replicate the hollow, lamellar vascular structure; demonstrated modeling potential using mechanical and chemical stimulation with a circulation flow system, an arterial surgery simulator, and cell co-culture	Gao et al. [112]
Bioink: Fibrin composites Sacrificial ink: Gelatin, glycerol, and hyaluronic acid	CM	Printed at 18C with a pneumatic pressure of 100 kPa and a speed of 100 mm/min; intrinsic force generated within printed construct was 1.5 mN	3D bioprinted organized and functional cardiac tissue; printed constructs elicited physiological responses to cardiac drugs to alter beating frequency and contractility forces	Wang et al. [137]
PGA-co-PLCL	Obtained through implantation	Burst pressure: 11,685 ± 11,506 mmHg (post-implant), 6167 ± 5627 mmHg (preoperative); Compliance: 4.0% ± 1.5% (preoperative), 2.3% ± 0.46% (post-implant)	Created a patient-specific nanofiber vascular graft combining electrospinning and 3D Printing; implanted in sheep, demonstrating no aneurysm formation or ectopic calcification; explanation revealed complete resorption of grafts, SMC organization, ECM deposition, endothelialization, and similar mechanical properties to native vasculature	Fukunishi et al. [153]
PEGDA and GelMA	HUVECs, NIH/3T3 Fibroblasts	Viscous bioink (Reynolds number ~ 10–100) permits for smooth transitions between bioinks; Printing resolution ~ 20–30 μm	Stereolithography-based, multi-material bioprinting platform for heterogeneous hydrogel constructs; Constructs loaded with VEGF were assessed for its neovascularization potential	Amir et al. [101]
GelMA and agarose	HepG2/C3A cells (encapsulated); HUVECs (seeded)	Youngs modulus of GelMA ~ 12.1 ± 1.1 kPa; pore size of GelMA ~ 143.2 ± 6.4 μm; perfusion was conducted at 50 μL h^{-1}	Sacrificial bioprinting technique produced hollow microchannels; HUVEC layer delayed permeability of biomolecules and showed increased viability of HEPG2/C3A cells	Massa et al. [102]

Abbreviations HUVECs, human umbilical vein endothelial cells; PEGDA, poly(ethylene glycol) diacrylate; GelMA, Gelatin Methacrylol; VEGF, vascular endothelial growth factor; hDFs, human dermal fibroblasts; hMSCs, human mesenchymal stem cells; CM, cardiomyocytes; PGA, polyglycolic acid; PLCL, poly(L-lactide-co-ε-caprolactone); PAVIC, porcine aortic valve interstitial cells.

practice. Specifically, lack of bioinks that can truly mimic the mechanical and chemical properties of the ECM is a big limiting factor. For example, there is no bioink that can provides an accurate representation of abnormal features observed in vascular diseases, such as calcified structures, mechanical and chemical variations within tissues, or differences in mechanical properties of vascular structures during dynamic or static states [93]. Moreover, biological arrangement of cells and tissues observed *in vivo* is challenging to control *in vitro*. Although use of electrospinning and other microfabrication technology along with 3D printing can be used to provide some control over cellular arrangement, this relies on cells innate ability to self-organize. Overall, 3D printing is promising new approach to mimic human vascular pathophysiology and have strong potential to dissect tissue-tissue and drug-tissue interactions for systematic analysis of complex vascular diseases.

6. Future prospects and conclusion

Multiscale modeling of vascular pathophysiology can provide molecular and cellular insights to understand complex biochemical and biophysical mechanisms of the human vascular system. The current gold standard consists of animal *in vivo* models and *in vitro* cell culture, however significant limitations persists in both these approaches as they are not able to recapitulate human pathophysiology. Recent developments in fabrication techniques, such as organ-on-chip and 3D printing, provide a unique solution to mimic human vascular function, thereby increasing the translational potential to humans and decreasing the mechanistic complexity associated with the experimental outputs. However, these emerging approaches are still in proof-of-concept stage and need further optimization to potentially aid in a better understanding of vascular pathophysiology while providing valuable tools for pharmaceutical research and translational outcomes. In order to utilize the full potential of organs-on-a-chip and 3D printing, as well as recapitulate critical aspects of vascular disease development and progression with high precision, the cell sources have to be primary and/or stem-cell derived. Human induced pluripotent stem cells (hiPSC) differentiated into targeted cell-lineages is an exciting new approach that may become the gold standard cell-source in these modeling systems in the future.

Table 4
Material properties of human vasculature and common vessel models.

Materials	Maximum Stress (MPa)	Maximum Strain	Elastic modulus (MPa)	Notes	Ref.
Healthy coronary artery	1.44 ± 0.87	0.54 ± 0.25	1.48 ± 0.24	Average age 38.07 ± 8.58; Strain rate of 1 mm/min	Karimi et al. [6]
Diseased coronary artery	2.08 ± 0.86	0.35 ± 0.11	3.77 ± 0.38	Average age 65.50 ± 10.33; Strain rate of 1 mm/min	Karimi et al. [6]
Layer-specific mechanical properties of coronary arteries	Adventitia: 1.43 ± 0.604 (circumferential) 1.3 ± 0.692 (longitudinal) Media: 0.446 ± 0.194 (circumferential) 0.419 ± 0.188 (longitudinal) Intima: 0.394 ± 0.223 (circumferential) 0.391 ± 0.144 (longitudinal)	Adventitia: 1.66 ± 0.24 (circumferential) 1.87 ± 0.38 (longitudinal) Media: 1.81 ± 0.37 (circumferential) 1.74 ± 0.28 (longitudinal) Intima: 1.6 ± 0.29 (circumferential) 1.55 ± 0.40 (longitudinal)	n.m.	Average age: 71.5 ± 7.3 years old	Holzapfel et al. [170]
Inferior vena cava	n.m.	n.m.	n.m.	Burst Pressure (mm Hg): 13,062 ± 6847 Compliance: 2.4% ± 0.85%	Fukunishi et al. [153]
Elastin/Collagen	0.5017 ± 0.3665	0.2855 ± 0.1210	Elastin: 0.49 ± 0.18 Collagen: 131 ± 64	Monfrel dogs aged 54.9 ± 8.8 months weighing at 20.4 ± 1.8 kg	Armentano et al. [171]
PDMS	5.39 ± 1.23	144 ± 9.3			Jang et al. [172]
PDMS	n.m.	n.m.	0.005–1.72	Increasing elastic moduli demonstrates higher surface roughness; Strain ranged from 0 to 10%	Palchesko et al. [173]
PDMS	n.m.	n.m.	2.04 ± 0.06 (10:1 PDMS:crosslinker) 0.42 ± 0.05 (30:1 PDMS:crosslinker)	0.1 N load with 0.01 mm displacement resolution; 10% strain applied to each sample at a rate of 0.25 mm s^{-1}	Carrillo et al. [174]
GelMA, κCA, & nSi (NICE)	0.3017 ± 0.021	70%	Tension: 0.495 ± 0.150 Compression: 0.0711 ± 0.0049	Demonstrated > 75% recovery after cyclic deformation	Chimene et al. [114]
GelMA	n.m.	n.m.	0.0005–0.001	Strain rate of 0.2 mm/min	Zhang et al. [75]
GelMA	n.m.	n.m.	0.0121 ± 0.0011	Tried to mimic vascularized liver (elastic modulus: 0.0055 ± 0.0016 MPa)	Massa et al. [102]
Sodium Alginate	0.049 ± 0.005 (2 wt%) to 0.184 ± 0.008 (4 wt%)	1.53 ± 0.10 (2 wt%) to 1.97 ± 0.009 (4 wt%)		Ramp force with a slope of 0.5 N min^{-1}	Gao et al. [112]
PEGDA (700 MW:8000 MW)	n.m.	20 wt% PEGDA 700: 0.50 ± 0.15 10 wt% PEGDA 8000: 1.6 ± 0.1	0.0053 ± 0.0009 (20 wt% PEGDA 700) to 0.0746 ± 0.0015 (10 wt% PEGDA 8000)	Loaded quasi-statically at 0.02 mm s^{-1} until failure with strain rate of 0.005 s^{-1}	Hockaday et al. [115]
PGA and PLCL	n.m.	n.m.	n.m.	Burst Pressure (mmHg): 6167 ± 5627 (pre-operative) 13,062 ± 6847 (6-months postoperative) Compliance: 4.0% ± 1.5% (preoperative) 2.3% ± 0.46% (postoperative)	Fukunishi et al. [153]
PLLA and SPEU-PHD	90/10 Outer-layer with 50/50 Inner-layer PLLA/PHD: 2.07 ± 0.17 (circumferential) 2.56 ± 0.28 (axial)	90/10 Outer-layer with 50/50 Inner-layer PLLA/PHD: 233.17 ± 34.62 (circumferential) 142.14 ± 23.87 (axial)	PLLA: 13.85 ± 3.82; 90/10 PLLA/PHD: 6.30 ± 0.75 50/50 PLLA/PHD: 5.35 ± 0.98 PHS: 0.56 ± 0.27; 90/10 Outer-layer with 50/50 Inner-layer PLLA/PHD: 6.24 ± 1.69 (circumferential) 29.54 ± 5.85 (axial)	Suture retention and burst pressure was dependent on thickness	Montini-Ballarin et al. [175]

Abbreviations n.a., not measured; PDMS, Polydimethylsiloxane; GelMA, Gelatin Methacrylate; κCA, κ-carrageenan; nSi, Nanosilicates; NICE, nanoengineered ionic-covalent entanglements; PEGDA, Poly(ethylene glycol) diacrylate; PGA, Polyglycolic acid; PLCL, Poly(L-lactide-co-ε-caprolactone); PLLA, Poly(L-lactic acid); SPEU-PHD, pigmented poly(ester urethane)-PHD.

Similarly, the physical properties of biomaterials need to be optimized in term of composition, stiffness, anisotropy, and permeability, all which impact vascular pathophysiology and disease development (Table 4). In addition, the materials used to fabricate vascular tissues should be able to withstand long-term cell culture for the assessment of disease progression (e.g. from the observation of EC dysfunction to stenosis, and eventually a plaque rupture). Bioinks and scaffold materials that provide structure to organs-on-chips and 3D bioprinted tissues can be enhanced with nanoengineered particles to improve their mechanical and biochemical functionality. Also, currently available fabrication techniques produce constructs that are not able to form vasculature geometries with anatomical accuracy. Some printers, such as the nanobiological printers, are able to provide resolutions up to 5–20 μm, however it is not evident if these features can be translated to extrusion-based printers using biological relevant, cell-laden bioinks [125]. Considering these geometrical constraints, there is a need for a printer that is able to construct multi-material,

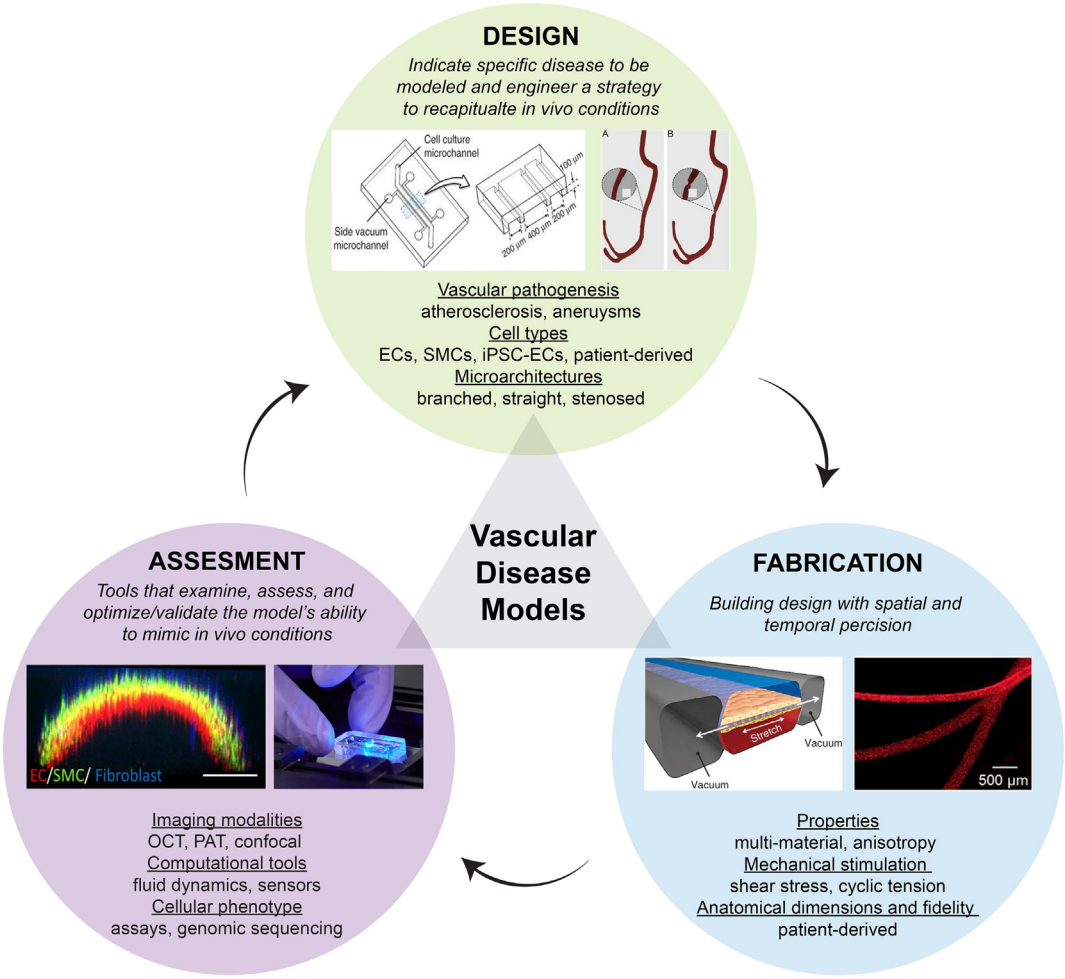

Fig. 5. The continuing cycle of model designs, fabrication techniques, and assessments/validations provides an engineered platform to mimic and test vascular physiology, functionalities, and response to drugs and toxins. Adapted images with permission from [160] © 2013 Nature Protocols [161] © 2017 American Chemical Society [162] © 2018 Advanced Functional Materials [163]© 2015 Nature [157] © 2018 American Chemical Society.

hierarchical structures across multiple length scales to mimic native vasculature. This will enable for the fabrication of heterogeneous tissue consisting of adventitia, media, and intima layers, all comprised of different cell-laden bioinks [112,157].

Given the increasing complexity of organ-on-a-chips and 3D printed structures, validation of the model to mimic *in vivo* conditions, such as cell phenotype and remodeling, are needed. Therefore, advanced imaging techniques, computational modeling, and the integration of genomics provide a means to further assess and validate engineered vascular models. Advanced imaging systems with enhanced penetration depth, such as optical coherence tomography (OCT) and photoacoustic tomography (PAT), would permit for visualization of the 3D structure and geometrical changes within the model. The use of more mature imaging modalities provides a means to non-invasively probe cell-cell and cell-matrix interactions when cultured within organ-on-a-chip devices and 3D printed models. In addition, emerging approaches also focus on the development of computational tools to model fluid dynamics, oxygen diffusion, cellular proliferation, remodeling, and viability within 3D models. This permits for researches to examine, assess, and optimize models prior to fabrication as well as correlate to *in vivo* observations. Furthermore, whole genome transcriptomic approaches can be applied to validate the cell behavior in response to materials to which they adhere to and to understand mechanistic pathways such that their function can be measured and designed for precision/personalized medicine [158].

In summary, the prospects of these emerging technologies are promising. The relationship between design, manufacturing, and assessment is closely related and never-ending, repeated cycle. Therefore, this process can be enhanced with bioengineering, material science, medicine, imaging, and genomic collaborations. Bringing these fields together will improve the success of these platforms to predict physiology and drug, toxin, and chemical responses at the patient level (Fig. 5) [159]. As more progress is made in this direction, organs-on-a-chip and 3D bioprinting technologies are expected to add new knowledge to vascular disease pathophysiology and predict therapeutic responses and toxicities to drugs at a disease- and patient-specific level that is impossible with animal models, thus directly impacting the entire healthcare system.

Acknowledgements

K.G. acknowledge financial support from Texas A&M University Graduate Diversity fellowship. A.K.G. would like to acknowledge financial support from the National Science Foundation (CBET 1705852), and the National Institutes of Health (DP2 EB026265, R03 EB023454). A.J. would like to acknowledge financial support

from Texas A&M Engineering Experiment Station (TEES) and Texas A&M University.

References

[1] D. Mozaffarian, E.J. Benjamin, A.S. Go, D.K. Arnett, M.J. Blaha, M. Cushman, S. de Ferranti, J.-P. Després, H.J. Fullerton, V.J. Howard, M.D. Huffman, S.E. Judd, B.M. Kissela, D.T. Lackland, J.H. Lichtman, L.D. Lisabeth, S. Liu, R.H. Mackey, D.B. Matchar, D.K. McGuire, E.R. Mohler, C.S. Moy, P. Muntner, M.E. Mussolino, K. Nasir, R.W. Neumar, G. Nichol, L. Palaniappan, D.K. Pandey, M.J. Reeves, C.J. Rodriguez, P.D. Sorlie, J. Stein, A. Towfighi, T.N. Turan, S.S. Virani, J.Z. Willey, D. Woo, R.W. Yeh, M.B. Turner, Heart disease and stroke Statistics—2015 update, Rep. Am. Heart Assoc. 131 (4) (2015) e29–e322.

[2] F. Wolf, F. Vogt, T. Schmitz-Rode, S. Jockenhoevel, P. Mela, Bioengineered vascular constructs as living models for in vitro cardiovascular research, Drug Discov. Today 21 (9) (2016) 1446–1455.

[3] S.B.T. Kinza Islam, Rasha Nasser, Deborah L. Gater, Tanthe E. Pearson, N. Christoforoul, Jeremy CM. Teo, Co-culture methods used to model atherosclerosis in vitro using endothelial, smooth muscle and monocyte cells, SM J. Biomed. Eng. 2 (1) (2016).

[4] A.H. Huang, J.L. Balestrini, B.V. Udelsman, K.C. Zhou, L. Zhao, J. Ferruzzi, B.C. Starcher, M.J. Levene, J.D. Humphrey, L.E. Niklason, Biaxial stretch improves elastic fiber maturation, collagen arrangement, and mechanical properties in engineered arteries, Tissue Eng. C Meth. 22 (6) (2016) 524–533.

[5] E. Claes, J.M. Atienza, G.V. Guinea, F.J. Rojo, J.M. Bernal, J.M. Revuelta, M. Elices, Mechanical properties of human coronary arteries, in: 2010 Annual International Conference of the IEEE Engineering in Medicine and Biology, 2010, pp. 3792–3795.

[6] A. Karimi, M. Navidbakhsh, A. Shojaei, S. Faghihi, Measurement of the uniaxial mechanical properties of healthy and atherosclerotic human coronary arteries, Mater. Sci. Eng. C 33 (5) (2013) 2550–2554.

[7] D.D. Gutterman, Adventitia-dependent influences on vascular function, Am. J. Physiol. Heart Circ. Physiol. 277 (4) (1999) H1265–H1272.

[8] S.S. Segal, Cell-to-cell communication coordinates blood flow control, Hypertension 23 (6 Pt 2) (1994) 1113–1120.

[9] Pathophysiology of Heart Disease: a Collaborative Project of Medical Students and Faculty, fourth ed., Lippincott Williams & Wilkins, Baltimore, MD, 2007.

[10] G.K. Hansson Inflammation, Atherosclerosis, and coronary artery disease, N. Engl. J. Med. 352 (16) (2005) 1685–1695.

[11] G.S. Hotamisligil, Endoplasmic reticulum stress and atherosclerosis, Nat. Med. 16 (4) (2010) 396–399.

[12] C. Weber, H. Noels, Atherosclerosis: current pathogenesis and therapeutic options, Nat. Med. 17 (11) (2011) 1410–1422.

[13] J.E. Wagenseil, R.P. Mecham, Vascular extracellular matrix and arterial mechanics, Physiol. Rev. 89 (3) (2009) 957–989.

[14] A.J. Ryan, C.M. Brougham, C.D. Garciarena, S.W. Kerrigan, F.J. O'Brien, Towards 3D in vitro models for the study of cardiovascular tissues and disease, Drug Discov. Today 21 (9) (2016) 1437–1445.

[15] R.S. Rosenson, H.B. Brewer Jr., P.J. Barter, J.L.M. Björkegren, M.J. Chapman, D. Gaudet, D.S. Kim, E. Niesor, K.-A. Rye, F.M. Sacks, J.-C. Tardif, R.A. Hegele, HDL and atherosclerotic cardiovascular disease: genetic insights into complex biology, Nat. Rev. Cardiol. 15 (2017) 9.

[16] K.-A. Rye, P.J. Barter, Regulation of high-density lipoprotein metabolism, Circ. Res. 114 (1) (2014) 143–156.

[17] G.A. Truskey, Endothelial cell vascular smooth muscle cell Co-Culture assay for high throughput screening assays for discovery of anti-angiogenesis agents and other therapeutic molecules, Int. J. High Throughput Screen. 2010 (1) (2010) 171–181.

[18] A. Persidis, Cardiovascular disease drug discovery, Nat. Biotechnol. 17 (1999) 930.

[19] G. Gromo, J. Mann, J.D. Fitzgerald, Cardiovascular drug discovery: a perspective from a research-based pharmaceutical company, Cold Spring Harbor Perspect. Med. 4 (6) (2014).

[20] T. Hampton, How useful are mouse models for understanding human atherosclerosis? Rev. Exam. Avail. Evid. 135 (18) (2017) 1757–1758.

[21] M. von Scheidt, Y. Zhao, Z. Kurt, C. Pan, L. Zeng, X. Yang, H. Schunkert, A.J. Lusis, Applications and limitations of mouse models for understanding human atherosclerosis, Cell Metabol. 25 (2) (2017) 248–261.

[22] J. Liao, W. Huang, G. Liu, Animal models of coronary heart disease, J. Biomed. Res. 31 (1) (2017) 3–10.

[23] G.S. Getz, C.A. Reardon, Animal models of atherosclerosis, Arterioscler. Thromb. Vasc. Biol. 32 (5) (2012) 1104–1115.

[24] P.F. Davies, Hemodynamic shear stress and the endothelium in cardiovascular pathophysiology, Nat. Clin. Pract. Cardiovasc. Med. 6 (1) (2009) 16–26.

[25] B. Emini Veseli, P. Perrotta, G.R.A. De Meyer, L. Roth, C. Van der Donckt, W. Martinet, G.R.Y. De Meyer, Animal models of atherosclerosis, Eur. J. Pharmacol. 816 (2017) 3–13.

[26] G. Hasenfuss, Animal models of human cardiovascular disease, heart failure and hypertrophy, Cardiovasc. Res. 39 (1) (1998) 60–76.

[27] J.C. Russell, S.D. Proctor, Small animal models of cardiovascular disease: tools for the study of the roles of metabolic syndrome, dyslipidemia, and atherosclerosis, Cardiovasc. Pathol. 15 (6) (2006) 318–330.

[28] B.C. Hansen, N.L. Bodkin, Primary prevention of diabetes mellitus by prevention of obesity in monkeys, Diabetes 42 (12) (1993) 1809–1814.

[29] B.C. Hansen, The metabolic syndrome x, Ann. N. Y. Acad. Sci. 892 (1) (1999) 1–24.

[30] I. Meyvantsson, D.J. Beebe, Cell culture models in microfluidic systems, Annu. Rev. Anal. Chem. 1 (1) (2008) 423–449.

[31] M.A. Farcas, L. Rouleau, R. Fraser, R.L. Leask, The development of 3-D, in vitro, endothelial culture models for the study of coronary artery disease, Biomed. Eng. Online 8 (1) (2009) 30.

[32] L. Rouleau, I.B. Copland, J.-C. Tardif, R. Mongrain, R.L. Leask, Neutrophil adhesion on endothelial cells in a novel asymmetric stenosis model: effect of wall shear stress gradients, Ann. Biomed. Eng. 38 (9) (2010) 2791–2804.

[33] L. Rouleau, J. Rossi, R.L. Leask, The response of human aortic endothelial cells in a stenotic hemodynamic environment: effect of duration, magnitude, and spatial gradients in wall shear stress, J. Biomech. Eng. 132 (7) (2010), 071015–071015-11.

[34] L. Rouleau, M. Farcas, J.-C. Tardif, R. Mongrain, R.L. Leask, Endothelial cell morphologic response to asymmetric stenosis hemodynamics: effects of spatial wall shear stress gradients, J. Biomech. Eng. 132 (8) (2010), 081013–081013-10.

[35] E.W.K. Young, M.W.L. Watson, S. Srigunapalan, A.R. Wheeler, C.A. Simmons, Technique for real-time measurements of endothelial permeability in a microfluidic membrane chip using laser-induced fluorescence detection, Anal. Chem. 82 (3) (2010) 808–816.

[36] P. Kolhar, A.C. Anselmo, V. Gupta, K. Pant, B. Prabhakarpandian, E. Ruoslahti, S. Mitragotri, Using shape effects to target antibody-coated nanoparticles to lung and brain endothelium, Proc. Natl. Acad. Sci. Unit. States Am. 110 (26) (2013) 10753–10758.

[37] N. Korin, M. Kanapathipillai, B.D. Matthews, M. Crescente, A. Brill, T. Mammoto, K. Ghosh, S. Jurek, S.A. Bencherif, D. Bhatta, A.U. Coskun, C.L. Feldman, D.D. Wagner, D.E. Ingber, Shear-activated nanotherapeutics for drug targeting to obstructed blood vessels, Science 337 (6095) (2012) 738–742.

[38] G. Lamberti, Y. Tang, B. Prabhakarpandian, Y. Wang, K. Pant, M.F. Kiani, B. Wang, Adhesive interaction of functionalized particles and endothelium in idealized microvascular networks, Microvasc. Res. 89 (2013) 107–114.

[39] N. Doshi, B. Prabhakarpandian, A. Rea-Ramsey, K. Pant, S. Sundaram, S. Mitragotri, Flow and adhesion of drug carriers in blood vessels depend on their shape: a study using model synthetic microvascular networks, J. Contr. Release 146 (2) (2010) 196–200.

[40] D.B. Cines, E.S. Pollak, C.A. Buck, J. Loscalzo, G.A. Zimmerman, R.P. McEver, J.S. Pober, T.M. Wick, B.A. Konkle, B.S. Schwartz, E.S. Barnathan, K.R. McCrae, B.A. Hug, A.-M. Schmidt, D.M. Stern, Endothelial cells in physiology and in the pathophysiology of vascular disorders, Blood 91 (10) (1998) 3527–3561.

[41] K. Jeong Ai, D.T. Nam, L. Zhen, Y. Fan, Z. Weilin, J.F. Mark, Brain endothelial hemostasis regulation by pericytes, J. Cerebr. Blood Flow Metabol. 26 (2) (2005) 209–217.

[42] D.S. Grant, K.-I. Tashiro, B. Segui-Real, Y. Yamada, G.R. Martin, H.K. Kleinman, Two different laminin domains mediate the differentiation of human endothelial cells into capillary-like structures in vitro, Cell 58 (5) (1989) 933–943.

[43] O. Morin, P. Patry, L. Lafleur, Heterogeneity of endothelial cells of adult rat liver as resolved by sedimentation velocity and flow cytometry, J. Cell. Physiol. 119 (3) (1984) 327–334.

[44] S. Sankar, N. Mahooti-Brooks, L. Bensen, T.L. McCarthy, M. Centrella, J.A. Madri, Modulation of transforming growth factor beta receptor levels on microvascular endothelial cells during in vitro angiogenesis, J. Clin. Invest. 97 (6) (1996) 1436–1446.

[45] G.W. Cockerill, K.-A. Rye, J.R. Gamble, M.A. Vadas, P.J. Barter, High-density lipoproteins inhibit cytokine-induced expression of endothelial cell adhesion molecules, Arterioscler. Thromb. Vasc. Biol. 15 (11) (1995) 1987–1994.

[46] C. Owman, J.E. Hardebo, Functional heterogeneity of the cerebrovascular endothelium, brain, Behavior and Evolution 32 (2) (1988) 65–75.

[47] M.H. Thornhill, D.O. Haskard, IL-4 regulates endothelial cell activation by IL-1, tumor necrosis factor, or IFN-gamma, J. Immunol. 145 (3) (1990) 865–872.

[48] M.F. Fillinger, L.N. Sampson, J.L. Cronenwett, R.J. Powell, R.J. Wagner, Coculture of endothelial cells and smooth muscle cells in bilayer and conditioned media models, J. Surg. Res. 67 (2) (1997) 169–178.

[49] G.K. Owens, M.S. Kumar, B.R. Wamhoff, Molecular regulation of vascular smooth muscle cell differentiation in development and disease, Physiol. Rev. 84 (2004).

[50] J.A. Beamish, P. He, K. Kottke-Marchant, R.E. Marchant, Molecular regulation of contractile smooth muscle cell phenotype: implications for vascular tissue engineering, Tissue Eng. B Rev. 16 (5) (2010) 467–491.

[51] K.E. Steucke, P.V. Tracy, E.S. Hald, J.L. Hall, P.W. Alford, Vascular smooth muscle cell functional contractility depends on extracellular mechanical properties, J. Biomech. 48 (12) (2015) 3044–3051.

[52] C.E. Fernandez, R.W. Yen, S.M. Perez, H.W. Bedell, T.J. Povsic, W.M. Reichert, G.A. Truskey, Human vascular microphysiological system for in vitro drug screening, Sci. Rep. 6 (2016) 21579.

[53] R.J. Powell, J.L. Cronenwett, M.F. Fillinger, R.J. Wagner, Effect of endothelial cells and transforming growth factor-ß1 on cultured vascular smooth muscle cell growth patterns, J. Vasc. Surg. 20 (5) (1994) 787–794.

[54] G.B. Nackman, F.R. Bech, M.F. Fillinger, R.J. Wagner, J.L. Cronenwett,

Endothelial cells modulate smooth muscle cell morphology by inhibition of transforming growth factor-beta1 activation, Surgery 120 (2) (1996) 418–426.
[55] M.J. Merrilees, L. Scott, Interaction of aortic endothelial and smooth muscle cells in culture Effect on glycosaminoglycan levels, Atherosclerosis 39 (2) (1981), 147–16.
[56] A. Skardal, T. Shupe, A. Atala, Organoid-on-a-chip and body-on-a-chip systems for drug screening and disease modeling, Drug Discov. Today 21 (9) (2016) 1399–1411.
[57] R.G. Bacabac, T.H. Smit, S.C. Cowin, J.J.W.A. Van Loon, F.T.M. Nieuwstadt, R. Heethaar, J. Klein-Nulend, Dynamic shear stress in parallel-plate flow chambers, J. Biomech. 38(1) 159–167.
[58] G.N. Bancroft, V.I. Sikavitsas, A.G. Mikos, Technical note: design of a flow perfusion bioreactor system for bone tissue-engineering applications, Tissue Eng. 9 (3) (2003) 549–554.
[59] J.M. Higgins, D.T. Eddington, S.N. Bhatia, L. Mahadevan, Sickle cell vaso-occlusion and rescue in a microfluidic device, Proc. Natl. Acad. Sci. Unit. States Am. 104 (51) (2007) 20496–20500.
[60] G. Barabino, L. McIntire, S. Eskin, D. Sears, M. Udden, Endothelial cell interactions with sickle cell, sickle trait, mechanically injured, and normal erythrocytes under controlled flow, Blood 70 (1) (1987) 152–157.
[61] G. Nash, C. Johnson, H. Meiselman, Rheologic impairment of sickle RBCs induced by repetitive cycles of deoxygenation-reoxygenation, Blood 72 (2) (1988) 539–545.
[62] E.W.K. Young, C.A. Simmons, Macro- and microscale fluid flow systems for endothelial cell biology, Lab a Chip 10 (2) (2010) 143–160.
[63] E.W.K. Young, D.J. Beebe, Fundamentals of microfluidic cell culture in controlled microenvironments, Chem. Soc. Rev. 39 (3) (2010) 1036–1048.
[64] L.G. Griffith, M.A. Swartz, Capturing complex 3D tissue physiology in vitro, Nat. Rev. Mol. Cell Biol. 7 (2006) 211.
[65] U.Y. Schaff, M.M.Q. Xing, K.K. Lin, N. Pan, N.L. Jeon, S.I. Simon, Vascular mimetics based on microfluidics for imaging the leukocyte-endothelial inflammatory response, Lab a Chip 7 (4) (2007) 448–456.
[66] D.E. Ingber, I. Tensegrity, Cell structure and hierarchical systems biology, J. Cell Sci. 116 (7) (2003) 1157–1173.
[67] D.E. Ingber, Tensegrity II, How structural networks influence cellular information processing networks, J. Cell Sci. 116 (8) (2003) 1397–1408.
[68] S. Yasotharan, S. Pinto, J.G. Sled, S.-S. Bolz, A. Gunther, Artery-on-a-chip platform for automated, multimodal assessment of cerebral blood vessel structure and function, Lab a Chip 15 (12) (2015) 2660–2669.
[69] J. Ribas, H. Sadeghi, A. Manbachi, J. Leijten, K. Brinegar, Y.S. Zhang, L. Ferreira, A. Khademhosseini, Cardiovascular organ-on-a-chip platforms for drug discovery and development, applied, In Vitro Toxicol. 2 (2) (2016) 82–96.
[70] A. Jain, A.D. van der Meer, A.-L. Papa, R. Barrile, A. Lai, B.L. Schlechter, M.A. Otieno, C.S. Louden, G.A. Hamilton, A.D. Michelson, A.L. Frelinger, D.E. Ingber, Assessment of whole blood thrombosis in a microfluidic device lined by fixed human endothelium, Biomed. Microdevices 18 (2016) 73.
[71] A. Jain, L.L. Munn, Biomimetic postcapillary expansions for enhancing rare blood cell separation on a microfluidic chip, Lab a Chip 11 (17) (2011) 2941–2947.
[72] A. Jain, A. Graveline, A. Waterhouse, A. Vernet, R. Flaumenhaft, D.E. Ingber, A shear gradient-activated microfluidic device for automated monitoring of whole blood haemostasis and platelet function, Nat. Commun. 7 (2016) 10176.
[73] K.H. Benam, S. Dauth, B. Hassell, A. Herland, A. Jain, K.-J. Jang, K. Karalis, H.J. Kim, L. MacQueen, R. Mahmoodian, S. Musah, Y.-s. Torisawa, A.D.v.d. Meer, R. Villenave, M. Yadid, K.K. Parker, D.E. Ingber, Engineered in vitro disease models, Annu. Rev. Pathol. 10 (1) (2015) 195–262.
[74] E. Westein, A.D. van der Meer, M.J.E. Kuijpers, J.-P. Frimat, A. van den Berg, J.W.M. Heemskerk, Atherosclerotic geometries exacerbate pathological thrombus formation poststenosis in a von Willebrand factor-dependent manner, Proc. Natl. Acad. Sci. Unit. States Am. 110 (4) (2013) 1357–1362.
[75] Y.S. Zhang, F. Davoudi, P. Walch, A. Manbachi, X. Luo, V. Dell'Erba, A.K. Miri, H. Albadawi, A. Arneri, X. Li, X. Wang, M.R. Dokmeci, A. Khademhosseini, R. Oklu, Bioprinted thrombosis-on-a-chip, Lab a Chip 16 (21) (2016) 4097–4105.
[76] L.E. Bertassoni, M. Cecconi, V. Manoharan, M. Nikkhah, J. Hjortnaes, A.L. Cristino, G. Barabaschi, D. Demarchi, M.R. Dokmeci, Y. Yang, A. Khademhosseini, Hydrogel bioprinted microchannel networks for vascularization of tissue engineering constructs, Lab a Chip 14 (13) (2014) 2202–2211.
[77] R. Barrile, A.D. van der Meer, H. Park, J.P. Fraser, D. Simic, F. Teng, D. Conegliano, J. Nguyen, A. Jain, M. Zhou, Organ-on-Chip recapitulates thrombosis induced by an anti-CD154 monoclonal antibody: translational potential of advanced microengineered systems, Clin. Pharmacol. Ther. (2018), https://doi.org/10.1002/bit.25160.
[78] S. Alimperti, T. Mirabella, V. Bajaj, W. Polacheck, D.M. Pirone, J. Duffield, J. Eyckmans, R.K. Assoian, C.S. Chen, Three-dimensional biomimetic vascular model reveals a RhoA, Rac1, and N-cadherin balance in mural cell–endothelial cell-regulated barrier function, Proc. Natl. Acad. Sci. Unit. States Am. 114 (33) (2017) 8758.
[79] A. Thomas, H. Daniel Ou-Yang, L. Lowe-Krentz, V.R. Muzykantov, Y. Liu, Biomimetic channel modeling local vascular dynamics of pro-inflammatory endothelial changes, Biomicrofluidics 10 (1) (2016), 014101.
[80] J.Y. Park, H.O. Kim, K.-D. Kim, S.K. Kim, S.K. Lee, H. Jung, Monitoring the status of T-cell activation in a microfluidic system, Analyst 136 (13) (2011) 2831–2836.
[81] S. Kim, H. Lee, M. Chung, N.L. Jeon, Engineering of functional, perfusable 3D microvascular networks on a chip, Lab a Chip 13 (8) (2013) 1489–1500.
[82] C.K. Fredrickson, Z.H. Fan, Macro-to-micro interfaces for microfluidic devices, Lab a Chip 4 (6) (2004) 526–533.
[83] G.M. Whitesides, The origins and the future of microfluidics, Nature 442 (2006) 368.
[84] R.W. Muthard, S.L. Diamond, Side view thrombosis microfluidic device with controllable wall shear rate and transthrombus pressure gradient, Lab a Chip 13 (10) (2013) 1883–1891.
[85] B.-h. Chueh, D. Huh, C.R. Kyrtsos, T. Houssin, N. Futai, S. Takayama, Leakage-Free bonding of porous membranes into layered microfluidic array systems, Anal. Chem. 79 (9) (2007) 3504–3508.
[86] Y.Y. Shery Huang, D. Zhang, Y. Liu, Bioprinting of three-dimensional culture models and organ-on-a-chip systems, MRS Bull. 42 (8) (2017) 593–599.
[87] X. Wang, D.T.T. Phan, A. Sobrino, S.C. George, C.C.W. Hughes, A.P. Lee, Engineering anastomosis between living capillary networks and endothelial cell-lined microfluidic channels, Lab a Chip 16 (2) (2016) 282–290.
[88] A. Memic, A. Navaei, B. Mirani, J.A.V. Cordova, M. Aldhahri, A. Dolatshahi-Pirouz, M. Akbari, M. Nikkhah, Bioprinting technologies for disease modeling, Biotechnol. Lett. 39 (9) (2017) 1279–1290.
[89] A.S. F2792–12A, Standard Terminology for Additive Manufacturing Technologies, ASTM International, 2013.
[90] X. Zhao, S.A. Irvine, A. Agrawal, Y. Cao, P.Q. Lim, S.Y. Tan, S.S. Venkatraman, 3D patterned substrates for bioartificial blood vessels – the effect of hydrogels on aligned cells on a biomaterial surface, Acta Biomater. 26 (2015) 159–168.
[91] S. Irvine, S. Venkatraman, Bioprinting and differentiation of stem cells, Molecules 21 (9) (2016) 1188.
[92] M. Bobak, X. Guanglei, D. Simon, K.M. James, Current progress in 3D printing for cardiovascular tissue engineering, Biomed. Mater. 10 (3) (2015), 034002.
[93] M. Vukicevic, B. Mosadegh, J.K. Min, S.H. Little, Cardiac 3D printing and its future directions, JACC (J. Am. Coll. Cardiol.): Cardiovasc. Imag. 10 (2) (2017) 171–184.
[94] G. Swati, B. Alpa, C. Manish, M. Shivaji, T. Bhadra, P.C. Vishal, S. Narayan, G. Sarang, A. Vijay, Clinical application and multidisciplinary assessment of three dimensional printing in double outlet right ventricle with remote ventricular septal defect, World J. Pedia. Congen. Heart Surg. 7 (3) (2016) 344–350.
[95] L.E. Niklason, J. Gao, W.M. Abbott, K.K. Hirschi, S. Houser, R. Marini, R. Langer, Functional arteries grown in vitro, Science 284 (5413) (1999) 489–493.
[96] K. Laflamme, C.J. Roberge, J. Labonté, S. Pouliot, P. D'Orléans-Juste, F.A. Auger, L. Germain, Tissue-engineered human vascular media with a functional endothelin system, Circulation 111 (4) (2005) 459–464.
[97] K. Laflamme, C.J. Roberge, G. Grenier, M. Rémy-Zolghadri, S. Pouliot, K. Baker, R. Labbé, P. D'Orléans-Juste, F.A. Auger, L. Germain, Adventitia contribution in vascular tone: insights from adventitia-derived cells in a tissue-engineered human blood vessel, Faseb. J. 20 (8) (2006) 1245–1247.
[98] M. Diebolt, K. Laflamme, R. Labbé, F.A. Auger, L. Germain, R. Andriantsitohaina, Polyphenols modulate calcium-independent mechanisms in human arterial tissue-engineered vascular media, J. Vasc. Surg. 46 (4) (2007) 764–772.
[99] M. Diebolt, L. Germain, F.A. Auger, R. Andriantsitohaina, Mechanism of potentiation by polyphenols of contraction in human vein-engineered media, Am. J. Physiol. Heart Circ. Physiol. 288 (6) (2005) H2918–H2924.
[100] M. Pricci, J.-M. Bourget, H. Robitaille, C. Porro, R. Soleti, H.A. Mostefai, F.A. Auger, M.C. Martinez, R. Andriantsitohaina, L. Germain, Applications of human tissue-engineered blood vessel models to study the effects of shed membrane microparticles from T-lymphocytes on vascular function, Tissue Eng. 15 (1) (2009) 137–145.
[101] M.A. K.N. Daniel, I. Luis, G.H. Hossein, M. Sushila, Ruiz-EsparzaG. U., K. Parastoo, M. Amir, D.M. Remzi, C. Shaochen, S.S. Ryon, Z.Y. Shrike, K. Ali, Microfluidics-enabled multimaterial maskless stereolithographic bioprinting, Adv. Mater., 0(0) 1800242.
[102] S. Massa, M. Sakr, J. Seo, P. Bandaru, A. Arneri, S. Bersini, E. Zare Eelanjegh, E. Jalilian, B.-H. Cha, S. Antona, A. Enrico, Y. Gao, S. Hassan, J. Acevedo, M. Dokmeci, Y. Zhang, A. Khademhosseini, S. Shin, Bioprinted 3D vascularized tissue model for drug toxicity analysis, Biomicrofluidics 11 (4) (2017), 044109.
[103] H.-W. Kang, S.J. Lee, I.K. Ko, C. Kengla, J.J. Yoo, A. Atala, A 3D bioprinting system to produce human-scale tissue constructs with structural integrity, Nat. Biotechnol. 34 (3) (2016) 312–319.
[104] G. Xiong, K. Kolli, H.A. Soohoo, J.K. Min, Abstract 19898: in-vitro assessment of coronary hemodynamics in 3D printed patient-specific geometry, Circulation 132 (Suppl 3) (2015). A19898–A19898.
[105] K.K. Kolli, J.K. Min, S. Ha, H. Soohoo, G. Xiong, Effect of varying hemodynamic and vascular conditions on fractional flow reserve: an in vitro study, J. Am. Heart Assoc. 5 (7) (2016).
[106] D.B. Kolesky, K.A. Homan, M.A. Skylar-Scott, J.A. Lewis, Three-dimensional bioprinting of thick vascularized tissues, Proc. Natl. Acad. Sci. Unit. States Am. 113 (12) (2016) 3179–3184.
[107] L. Ouyang, C.B. Highley, C.B. Rodell, W. Sun, J.A. Burdick, 3D printing of shear-thinning hyaluronic acid hydrogels with secondary cross-linking, ACS Biomater. Sci. Eng. 2 (10) (2016) 1743–1751.

[108] M. Itoh, K. Nakayama, R. Noguchi, K. Kamohara, K. Furukawa, K. Uchihashi, S. Toda, J.-i. Oyama, K. Node, S. Morita, Scaffold-Free tubular tissues created by a Bio-3D printer undergo remodeling and endothelialization when implanted in rat aortae, PLoS One 10 (9) (2015), e0136681.
[109] K. Iwasaki, K. Kojima, S. Kodama, A.C. Paz, M. Chambers, M. Umezu, C.A. Vacanti, Bioengineered three-layered robust and elastic artery using hemodynamically-equivalent pulsatile bioreactor, Circulation 118 (14 suppl 1) (2008) S52–S57.
[110] K.J. Tsai, S. Dixon, L.R. Hale, A. Darbyshire, D. Martin, A. de Mel, Biomimetic heterogenous elastic tissue development, npj Regen. Med. 2 (1) (2017) 16.
[111] J.K. Carrow, P. Kerativitayanan, M.K. Jaiswal, G. Lokhande, A.K. Gaharwar, Chapter 13-polymers for bioprinting a2-atala, anthony, in: J.J. Yoo (Ed.), Essentials of 3D Biofabrication and Translation, Academic Press, Boston, 2015, pp. 229–248.
[112] Q. Gao, Z. Liu, Z. Lin, J. Qiu, Y. Liu, A. Liu, Y. Wang, M. Xiang, B. Chen, J. Fu, Y. He, 3D bioprinting of vessel-like structures with multilevel fluidic channels, ACS Biomater. Sci. Eng. 3 (3) (2017) 399–408.
[113] C.W. Peak, J. Stein, K.A. Gold, A.K. Gaharwar, Nanoengineered colloidal inks for 3D bioprinting, Langmuir 34 (3) (2018) 917–925.
[114] D. Chimene, C.W. Peak, J.L. Gentry, J.K. Carrow, L.M. Cross, E. Mondragon, G.B. Cardoso, R. Kaunas, A.K. Gaharwar, Nanoengineered ionic–covalent entanglement (NICE) bioinks for 3D bioprinting, ACS Appl. Mater. Interfaces 10 (12) (2018) 9957–9968.
[115] L.A. Hockaday, K.H. Kang, N.W. Colangelo, P.Y.C. Cheung, B. Duan, E. Malone, J. Wu, L.N. Girardi, L.J. Bonassar, H. Lipson, C.C. Chu, J.T. Butcher, Rapid 3D printing of anatomically accurate and mechanically heterogeneous aortic valve hydrogel scaffolds, Biofabrication 4 (3) (2012), 035005.
[116] H. Xiaoxiao, B. Richard, H. Russell, Engineering design of artificial vascular junctions for 3D printing, Biofabrication 8 (2) (2016), 025018.
[117] S.R. Shin, S.M. Jung, M. Zalabany, K. Kim, P. Zorlutuna, S.b. Kim, M. Nikkhah, M. Khabiry, M. Azize, J. Kong, K.-t. Wan, T. Palacios, M.R. Dokmeci, H. Bae, X. Tang, A. Khademhosseini, Carbon-nanotube-embedded hydrogel sheets for engineering cardiac constructs and bioactuators, ACS Nano 7 (3) (2013) 2369–2380.
[118] M. Izadifar, D. Chapman, P. Babyn, X. Chen, M.E. Kelly, Uv-assisted 3D bioprinting of nanoreinforced hybrid cardiac patch for myocardial tissue engineering, Tissue Eng. C Meth. 24 (2) (2017) 74–88.
[119] A. Paul, A. Hasan, H.A. Kindi, A.K. Gaharwar, V.T.S. Rao, M. Nikkhah, S.R. Shin, D. Krafft, M.R. Dokmeci, D. Shum-Tim, A. Khademhosseini, Injectable graphene oxide/hydrogel-based angiogenic gene delivery system for vasculogenesis and cardiac repair, ACS Nano 8 (8) (2014) 8050–8062.
[120] A. Navaei, H. Saini, W. Christenson, R.T. Sullivan, R. Ros, M. Nikkhah, Gold nanorod-incorporated gelatin-based conductive hydrogels for engineering cardiac tissue constructs, Acta Biomater. 41 (2016) 133–146.
[121] S.A. Wilson, L.M. Cross, C.W. Peak, A.K. Gaharwar, Shear-thinning and thermo-reversible nanoengineered inks for 3D bioprinting, ACS Appl. Mater. Interfaces 9 (50) (2017) 43449–43458.
[122] D. Chimene, D.L. Alge, A.K. Gaharwar, Two-dimensional nanomaterials for biomedical applications: emerging trends and future prospects, Adv. Mater. 27 (45) (2015) 7261–7284.
[123] L.M. Cross, K. Shah, S. Palani, C.W. Peak, A.K. Gaharwar, Gradient nanocomposite hydrogels for interface tissue engineering, Nanomed. Nanotechnol. Biol. Med. (2017), https://doi.org/10.1016/j.nano.2017.02.022.
[124] G. Lokhande, J.K. Carrow, T. Thakur, J.R. Xavier, M. Parani, K.J. Bayless, A.K. Gaharwar, Nanoengineered injectable hydrogels for wound healing application, Acta Biomater. 70 (2018) 35–47.
[125] S.V. Murphy, A. Atala, 3D bioprinting of tissues and organs, Nat. Biotechnol. 32 (2014) 773.
[126] B.C. Streifel, J.G. Lundin, A.M. Sanders, K.A. Gold, T.S. Wilems, S.J. Williams, E. Cosgriff-Hernandez, J.H. Wynne, Hemostatic and absorbent PolyHIPE–Kaolin composites for 3D printable wound dressing materials, Macromol. Biosci. 18 (5) (2018), 1700414.
[127] N.A. Sears, P.S. Dhavalikar, E.M. Cosgriff-Hernandez, Emulsion inks for 3D printing of high porosity materials, Macromol. Rapid Commun. 37 (16) (2016) 1369–1374.
[128] H. Ding, R. Chang, Printability study of bioprinted tubular structures using liquid hydrogel precursors in a support bath, Appl. Sci. 8 (3) (2018) 403.
[129] Y. Jin, W. Chai, Y. Huang, Printability study of hydrogel solution extrusion in nanoclay yield-stress bath during printing-then-gelation biofabrication, Mater. Sci. Eng. C 80 (2017) 313–325.
[130] Y. Jin, A. Compaan, W. Chai, Y. Huang, Functional nanoclay suspension for printing-then-solidification of liquid materials, ACS Appl. Mater. Interfaces 9 (23) (2017) 20057–20066.
[131] M. Rocca, A. Fragasso, W. Liu, M.A. Heinrich, Y.S. Zhang, Embedded multimaterial extrusion bioprinting, Slas Technol.: Trans. Life Sci. Innov., 0(0) 2472630317742071.
[132] D. Chimene, K.K. Lennox, R.R. Kaunas, A.K. Gaharwar, Advanced bioinks for 3D printing: a materials science perspective, Ann. Biomed. Eng. 44 (6) (2016) 2090–2102.
[133] J. Jang, H.-J. Park, S.-W. Kim, H. Kim, J.Y. Park, S.J. Na, H.J. Kim, M.N. Park, S.H. Choi, S.H. Park, S.W. Kim, S.-M. Kwon, P.-J. Kim, D.-W. Cho, 3D printed complex tissue construct using stem cell-laden decellularized extracellular matrix bioinks for cardiac repair, Biomaterials 112 (2017) 264–274.
[134] B. Weining, P.J. Christopher, B. Nenad, Controlling the structural and functional anisotropy of engineered cardiac tissues, Biofabrication 6 (2) (2014), 024109.
[135] M.O. Wang, C.E. Vorwald, M.L. Dreher, E.J. Mott, M.-H. Cheng, A. Cinar, H. Mehdizadeh, S. Somo, D. Dean, E.M. Brey, J.P. Fisher, Evaluating 3D printed biomaterials as scaffolds for vascularized bone tissue engineering, Adv. Mater. (Deerfield Beach, Fla.) 27 (1) (2015) 138–144.
[136] T. Ajay, I. Scott Alexander, S. Udi, M. Priyadarshini, B. Vrushali, V. Subbu, Contact guidance for cardiac tissue engineering using 3D bioprinted gelatin patterned hydrogel, Biofabrication 10 (2) (2018), 025003.
[137] Z. Wang, S.J. Lee, H.-J. Cheng, J.J. Yoo, A. Atala, 3D bioprinted functional and contractile cardiac tissue constructs, Acta Biomater. 70 (2018) 48–56.
[138] S.L. Cooper, N.A. Peppas, A.S. Hoffman, B.D. Ratner, Biomaterials: Interfacial Phenomena and Applications, American Chemical Society, 1982.
[139] R. Daniel, J. Wenkai, S. Dhavan, F. Kemin, W. Guifang, G. Jeremy, Z. Feng, Tissue engineering at the blood-contacting surface: a review of challenges and strategies in vascular graft development, Adv. Healthcare Mater., 0(0) 1701461.
[140] S. Sandip, K.M. Sales, H. George, S.A. Seifalian, Addressing thrombogenicity in vascular graft construction, J. Biomed. Mater. Res. B Appl. Biomater. 82B (1) (2007) 100–108.
[141] M. Hulander, A. Lundgren, L. Faxälv, T.L. Lindahl, A. Palmquist, M. Berglin, H. Elwing, Gradients in surface nanotopography used to study platelet adhesion and activation, Colloids Surfaces B Biointerfaces 110 (2013) 261–269.
[142] J.F. Hecker, R.O. Edwards, Effects of roughness on the thrombogenicity of a plastic, J. Biomed. Mater. Res. 15 (1) (1981) 1–7.
[143] V. Milleret, T. Hefti, H. Hall, V. Vogel, D. Eberli, Influence of the fiber diameter and surface roughness of electrospun vascular grafts on blood activation, Acta Biomater. 8 (12) (2012) 4349–4356.
[144] M.F. Kee, D.R. Myers, Y. Sakurai, W.A. Lam, Y. Qiu, Platelet mechanosensing of collagen matrices, PLoS One 10 (4) (2015), e0126624.
[145] Y. Qiu, A.C. Brown, D.R. Myers, Y. Sakurai, R.G. Mannino, R. Tran, B. Ahn, E.T. Hardy, M.F. Kee, S. Kumar, G. Bao, T.H. Barker, W.A. Lam, Platelet mechanosensing of substrate stiffness during clot formation mediates adhesion, spreading, and activation, Proc. Natl. Acad. Sci. Unit. States Am. 111 (40) (2014) 14430–14435.
[146] Y. Qiu, J. Ciciliano, D.R. Myers, R. Tran, W.A. Lam, Platelets and physics: how platelets "feel" and respond to their mechanical microenvironment, Blood Rev. 29 (6) (2015) 377–386.
[147] W.F. Daamen, J.H. Veerkamp, J.C.M. van Hest, T.H. van Kuppevelt, Elastin as a biomaterial for tissue engineering, Biomaterials 28 (30) (2007) 4378–4398.
[148] V.A. Kumar, J.M. Caves, C.A. Haller, E. Dai, L. Liu, S. Grainger, E.L. Chaikof, Acellular vascular grafts generated from collagen and elastin analogs, Acta Biomater. 9 (9) (2013) 8067–8074.
[149] G. Anna, B.Y. Han, J. Harvey, M. Fazal, M. Donald, F. Jan, K.S. Wan, Heparin release from thermosensitive polymer coatings: in vivo studies, J. Biomed. Mater. Res. 29 (7) (1995) 811–821.
[150] Y. Li, K.G. Neoh, E.T. Kang, Controlled release of heparin from polypyrrole-poly(vinyl alcohol) assembly by electrical stimulation, J. Biomed. Mater. Res. 73A (2) (2005) 171–181.
[151] M. Kharaziha, A. Memic, M. Akbari, D.A. Brafman, M. Nikkhah, Nano-enabled approaches for stem cell-based cardiac tissue engineering, Adv. Healthcare Mater. 5 (13) (2016) 1533–1553.
[152] N. Thavandiran, S.S. Nunes, Y. Xiao, M. Radisic, Topological and electrical control of cardiac differentiation and assembly, Stem Cell Res. Ther. 4 (1) (2013) 14.
[153] T. Fukunishi, C.A. Best, T. Sugiura, J. Opfermann, C.S. Ong, T. Shinoka, C.K. Breuer, A. Krieger, J. Johnson, N. Hibino, Preclinical study of patient-specific cell-free nanofiber tissue-engineered vascular grafts using 3-dimensional printing in a sheep model, J. Thorac. Cardiovasc. Surg. 153 (4) (2017) 924–932.
[154] D.B. Kolesky, R.L. Truby, A.S. Gladman, T.A. Busbee, K.A. Homan, J.A. Lewis, 3D bioprinting of vascularized, heterogeneous cell-laden tissue constructs, Adv. Mater. 26 (19) (2014) 3124–3130.
[155] W. Wu, C.J. Hansen, A.M. Aragon, P.H. Geubelle, S.R. White, J.A. Lewis, Direct-write assembly of biomimetic microvascular networks for efficient fluid transport, Soft Matter 6 (4) (2010) 739–742.
[156] W. Willie, D. Adam, J.A. Lewis, Omnidirectional printing of 3D microvascular networks, Adv. Mater. 23 (24) (2011) H178–H183.
[157] L. Ouyang, J.A. Burdick, W. Sun, Facile biofabrication of heterogeneous multilayer tubular hydrogels by fast diffusion-induced gelation, ACS Appl. Mater. Interfaces 10 (15) (2018) 12424–12430.
[158] J.K. Carrow, L.M. Cross, R.W. Reese, M.K. Jaiswal, C.A. Gregory, R. Kaunas, I. Singh, A.K. Gaharwar, Widespread changes in transcriptome profile of human mesenchymal stem cells induced by two-dimensional nanosilicates, Proc. Natl. Acad. Sci. Unit. States Am. 115 (17) (2018) E3905–E3913.
[159] E.A. Makris, A.H. Gomoll, K.N. Malizos, J.C. Hu, K.A. Athanasiou, Repair and tissue engineering techniques for articular cartilage, Nat. Rev. Rheumatol. 11 (2014) 21.
[160] D. Huh, H.J. Kim, J.P. Fraser, D.E. Shea, M. Khan, A. Bahinski, G.A. Hamilton, D.E. Ingber, Microfabrication of human organs-on-chips, Nat. Protoc. 8 (2013) 2135.
[161] P.F. Costa, H.J. Albers, J.E.A. Linssen, H.H.T. Middelkamp, L. van der Hout, R. Passier, A. van den Berg, J. Malda, A.D. van der Meer, Mimicking arterial thrombosis in a 3D-printed microfluidic in vitro vascular model based on computed tomography angiography data, Lab a Chip 17 (16) (2017)

2785–2792.
[162] S. Massa, M.A. Sakr, J. Seo, P. Bandaru, A. Arneri, S. Bersini, E. Zare-Eelanjegh, E. Jalilian, B-H Cha, S. Antona, A. Enrico, Y. Gao, S. Hassan, J.P. Acevedo, M.R. Dokmeci, Y.S. Zhang, A. Khademhosseini, S.R. Shin, Bioprinted 3D vascularized tissue model for drug toxicity analysis, Biomicrofluidics 11 (044109) (2017) 1–9.
[163] S. Reardon, 'Organs-on-chips' go mainstream, Nature 523 (2015).
[164] Y. Qiu, B. Ahn, Y. Sakurai, C.E. Hansen, R. Tran, P.N. Mimche, R.G. Mannino, J.C. Ciciliano, T.J. Lamb, C.H. Joiner, S.F. Ofori-Acquah, W.A. Lam, Microvasculature-on-a-chip for the long-term study of endothelial barrier dysfunction and microvascular obstruction in disease, Nature Biomedical Engineering 2 (6) (2018) 453–463.
[165] S. Alimperti, T. Mirabella, V. Bajaj, W. Polacheck, D.M. Pirone, J. Duffield, J. Eyckmans, R.K. Assoian, C.S. Chen, Three-dimensional biomimetic vascular model reveals a RhoA, Rac1, and N-cadherin balance in mural cell–endothelial cell-regulated barrier function, Proc. Natl. Acad. Sci. Unit. States Am. 114 (33) (2017) 8758–8763.
[166] A. Gunther, S. Yasotharan, A. Vagaon, C. Lochovsky, S. Pinto, J. Yang, C. Lau, J. Voigtlaender-Bolz, S.-S. Bolz, A microfluidic platform for probing small artery structure and function, Lab a Chip 10 (18) (2010) 2341–2349.
[167] A. Jain, R. Barrile, A.D. van der Meer, A. Mammoto, T. Mammoto, K. De Ceunynck, O. Aisiku, M.A. Otieno, C.S. Louden, G.A. Hamilton, R. Flaumenhaft, D.E. Ingber, A primary human lung alveolus-on-a-chip model of intravascular thrombosis for assessment of therapeutics, Clin. Pharmacol. Ther. 103 (2018) 332–340, https://doi.org/10.1002/cpt.742.
[168] C.N. Janna, L.S. Lisa, T.H. Ryan, T. Jason, P.F. John Jr., P.S. Sean, C. Alex, K. Suraj, S. Ilona, A.G. Josue, H.C. Patrick, P. Kevin Kit, Automated fabrication of photopatterned gelatin hydrogels for organ-on-chips applications, Biofabrication 10 (2) (2018), 025004.
[169] N.C.A. van Engeland, A.M.A.O. Pollet, J.M.J. den Toonder, C.V.C. Bouten, O.M.J.A. Stassen, C.M. Sahlgren, A biomimetic microfluidic model to study signalling between endothelial and vascular smooth muscle cells under hemodynamic conditions, Lab a Chip 18 (11) (2018) 1607–1620.
[170] G.A. Holzapfel, G. Sommer, C.T. Gasser, P. Regitnig, Determination of layer-specific mechanical properties of human coronary arteries with non-atherosclerotic intimal thickening and related constitutive modeling, Am. J. Physiol. Heart Circ. Physiol. 289 (5) (2005) H2048–H2058.
[171] R.L. Armentano, J. Levenson, J.G. Barra, E.I. Fischer, G.J. Breitbart, R.H. Pichel, A. Simon, Assessment of elastin and collagen contribution to aortic elasticity in conscious dogs, Am. J. Physiol. Heart Circ. Physiol. 260 (6) (1991) H1870–H1877.
[172] S.-H. Jang, Y.-L. Park, H. Yin, Influence of coalescence on the anisotropic mechanical and electrical properties of nickel powder/polydimethylsiloxane composites, Materials 9 (4) (2016) 239.
[173] R.N. Palchesko, L. Zhang, Y. Sun, A.W. Feinberg, Development of polydimethylsiloxane substrates with tunable elastic modulus to study cell mechanobiology in muscle and nerve, PLoS One 7 (12) (2012), e51499.
[174] F. Carrillo, S. Gupta, M. Balooch, S.J. Marshall, G.W. Marshall, L. Pruitt, C.M. Puttlitz, Nanoindentation of polydimethylsiloxane elastomers: effect of crosslinking, work of adhesion, and fluid environment on elastic modulus, J. Mater. Res. 20 (10) (2011) 2820–2830.
[175] F. Montini-Ballarin, D. Calvo, P.C. Caracciolo, F. Rojo, P.M. Frontini, G.A. Abraham, G.V. Guinea, Mechanical behavior of bilayered small-diameter nanofibrous structures as biomimetic vascular grafts, J. Mech. Behav. Biomed. Mater. 60 (2016) 220–233.